Sea Surface Temperature in the Northwest Atlantic—Space and Time Scales, Spectra and Spatially Smoothed Fields

R.H. Loucks, K.R. Thompson, and R.W. Trites

Published by:
Marine Ecology Laboratory
Department of Fisheries and Oceans

Bedford Institute of Oceanography
P.O. Box 1006
Dartmouth, Nova Scotia B2Y 4A2

April 1986

Canadian Technical Report of Fisheries and Aquatic Sciences No. 1430

Canadian Technical Report of Fisheries and Aquatic Sciences

These reports contain scientific and technical information that represents an important contribution to existing knowledge but which for some reason may not be appropriate for primary scientific (i.e. *Journal*) publication. Technical Reports are directed primarily towards a worldwide audience and have an international distribution. No restriction is placed on subject matter and the series reflects the broad interests and policies of the Department of Fisheries and Oceans, namely, fisheries management, technology and development, ocean sciences, and aquatic environments relevant to Canada.

Technical Reports may be cited as full publications. The correct citation appears above the abstract of each report. Each report will be abstracted in *Aquatic Sciences and Fisheries Abstracts* and will be indexed annually in the Department's index to scientific and technical publications.

Numbers 1-456 in this series were issued as Technical Reports of the Fisheries Research Board of Canada. Numbers 457-714 were issued as Department of the Environment, Fisheries and Marine Service, Research and Development Directorate Technical Reports. Numbers 715-924 were issued as Department of Fisheries and the Environment, Fisheries and Marine Service Technical Reports. The current series name was changed with report number 925.

Details on the availability of Technical Reports in hard copy may be obtained from the issuing establishment indicated on the front cover.

Rapport technique canadien des sciences halieutiques et aquatiques

Ces rapports contiennent des renseignements scientifiques et techniques qui constituent une contribution importante aux connaissances actuelles mais qui, pour une raison ou pour une autre, ne semblent pas appropriés pour la publication dans un journal scientifique. Il n'y a aucune restriction quant au sujet, de fait, la série reflète la vaste gamme des intérêts et des politiques du Ministère des Pêches et des Océans, notamment gestion des pêches, techniques et développement, sciences océaniques et environnements aquatiques, au Canada.

Les Rapports techniques peuvent être considérés comme des publications complètes. Le titre exact paraîtra au haut du résumé de chaque rapport, qui sera publié dans la revue *Aquatic Sciences and Fisheries Abstracts* et qui figurera dans l'index annuel des publications scientifiques et techniques du Ministère.

Les numéros 1-456 de cette série ont été publiés à titre de Rapports techniques de l'Office des recherches sur les pêcheries du Canada. Les numéros 457-714, à titre de Rapports techniques de la Direction générale de la recherche et du développement, Service des pêches et de la mer, ministère de l'Environnement. Les numéros 715-924 ont été publiés à titre de Rapports techniques du Service des pêches et de la mer, Ministère des Pêches et de l'Environnement. Le nom de la série a été modifié à partir du numéro 925.

La page couverture porte le nom de l'établissement auteur où l'on peut se procurer les rapports sous couverture cartonnée.

Canadian Technical Report of

Fisheries and Aquatic Sciences 1430

April 1986

SEA SURFACE TEMPERATURE IN THE NORTHWEST ATLANTIC - SPACE AND TIME SCALES, SPECTRA AND SPATIALLY SMOOTHED FIELDS

by

R. H. Loucks[1], K.R. Thompson[2] and R. W. Trites[3]

This is the 93rd Technical Report from the

Marine Ecology Laboratory, Dartmouth, N.S.

[1] R. H. Loucks Oceanology Limited, 24 Clayton Park Drive, Halifax, Nova Scotia.

[2] Department of Oceanography, Dalhousie University, Halifax, Nova Scotia.

[3] Department of Fisheries and Oceans, Marine Ecology Laboratory, Bedford Institute of Oceanography, Dartmouth, Nova Scotia.

©Minister of Supply and Services Canada 1986

Cat. No. Fs 97-6/1430E ISSN 0706-6457

Correct citation for this publication:

Loucks, R.H., K. R. Thompson, and R. W. Trites. 1986. Sea surface temperature in the northwest Atlantic - space and time scales, spectra and spatially smoothed fields. Can. Tech. Rep. Fish. Aquat. Sci. 1430 : 80 p.

ABSTRACT

Loucks, R.H., K.R. Thompson, and R.W. Trites. 1986. Sea surface temperatures in the northwest Atlantic - space and time scales, spectra and spatially smoothed fields. Can. Tech. Rep. Fish. Aquat. Sci. 1430 : 80 p.

A hypothesis for the organization of forcing mechanisms affecting anomalies of sea surface temperatures (SST's) is presented. The SST anomaly field for the Northwestern Atlantic over the period, 1946-1980, is described; space scales are revealed using empirical orthogonal function (EOF) analysis; temporal scales are determined using cross-spectra. The cross-spectra are further utilized in a complex EOF analysis for propagating 'waves' of SST anomalies. The EOF modes are used to achieve a spatial smoothing of the SST field which facilitates interpretation. Finally, the characteristics of the SST field are compared with those of the candidate forcing mechanisms, as hypothesized.

RÉSUMÉ

Loucks, R.H., K.R. Thompson, and R.W. Trites. 1986. Sea surface temperatures in the northwest Atlantic - space and time scales, spectra and spatially smoothed fields. Can. Tech. Rep. Fish. Aquat. Sci. 1430 : 80 p.

On présente une hypothèse d'organisation des mécanismes qui déterminent les anomalies de température de surface de la mer (TSM). On décrit le champ d'anomalies de TSM dans le nord-ouest de l'Atlantique entre 1946 et 1980; on évalue leur étendue au moyen d'une analyse de fonctions orthogonales empiriques (FOE) et leur durée au moyen de spectres croisés. On introduit ensuite les spectres croisés dans une analyse de FOE complexes pour établir des "ondes" de propagation des anomalies de TSM. Les FOE servent à réaliser un lissage spatial du champ de TSM qui facilite l'interprétation. Enfin, on compare les caractéristiques du champ de TSM à celles des mécanismes retenus selon l'hypothèse.

TABLE OF CONTENTS

ABSTRACT 3

INTRODUCTION 5

PROCEDURE 5

RESULTS AND DISCUSSION 7

THE SEASONAL CYCLE IN SST'S 7
MONTHLY ANOMALIES IN COMPARISON TO SUMMER-WINTER DIFFERENCES 8
SPATIAL SCALES OF THE ANOMALY FIELD 9
TEMPORAL SCALES OF THE ANOMALY FIELD 11
Seasonal Variances 11
Time Series 12
Spectra 12
CEOF's 15
Summary 16
RECONSTRUCTION OF THE SST FIELDS FROM EOF MODES 17
Reconstruction Technique 17
Results on a yearly time scale, 1950-52 & 1964-66 19
Results on a scale of months 21
HYPOTHESIS 23

CONCLUSIONS 24

REFERENCES 28

ACKNOWLEDGEMENTS 28

TABLES 30

FIGURES 32

APPENDICES 70

A. EOF ANALYSIS 70
B. RELATIONSHIP BETWEEN SST ANOMALY FIELD AND WIND 73
C. RELATIONSHIP BETWEEN SST ANOMALY AND RIVER RUNOFF 76
D. RELATIONSHIP BETWEEN SST ANOMALY FIELD AND OFFSHORE FORCING 77

INTRODUCTION

We have had a continuing interest in utilizing the SST information derived principally from cooling water intake measurements on merchant vessels known as the 'Marine Deck', for describing the SST field of the Northwest Atlantic and extending our results to applications in climatology and fisheries research. In particular, we have focussed on the between-year variability of SST's for selected areas - fishing banks and oceanographic features in the Northwest Atlantic (Figure 1) (see also Loucks and Trites, 1985, hereafter referred to as LT). In this report we discuss the spatial and temporal scales of the monthly anomalies of SST, their spectra, and a spatially-smoothed version of the SST field. This will set the stage for discussion of the possible relationship of SST's with the large-scale weather patterns, river runoff and offshore forcing.

Figure 2 is a schematic of hypothesized linkages between SST anomalies, meteorological, river runoff, and offshore effects. This working hypothesis was described in LT and Trites and Loucks (1985) and will be used in suggesting interpretations for the new results in this paper.

PROCEDURE

As recounted in LT, monthly average and median SST's were calculated for the selected areas from ships' weather reports for the period 1940 to 1980 although to avoid the war years when data tended to be sparse these analyses were based on the period 1946 to 1980. The medians were utilized as protection (in addition to automated and manual editing) against erroneous entries in the data base. The monthly medians and their anomalies from long term averages were plotted. For months with no observations in a particular area, the long term monthly mean was substituted. In cases where the anomaly was very large (> 4 degrees Celsius) and either the number of supporting observations was very small or the standard

deviation of observed SST's was very large (>4 Celsius degrees), the computed median was replaced with an interpolated value. The few such substitutions required were made mostly for northern areas where data tend to be sparser.

The primary technique used is that of empirical orthogonal function (EOF) analysis, both ordinary (OEOF) and complex (CEOF). The OEOF technique can be thought of as extracting from the SST field first the single combination of area signals which captures the maximum fraction of the variance in the field (mode 1), and second the combination (mode 2), orthogonal to the first, which most efficiently extracts variance from the remainder, and so forth. The orthogonality condition is seminal: there is the advantage that the modes are uncorrelated (at zero lag); and the disadvantage that, where SST anomalies are set-up in response to forcing mechanisms which are themselves related, the first mode will reflect contributions from all related components. This can severely complicate physical interpretation of the modes.

The OEOF modes or patterns are based on covariance or correlation matrices and represent, in a sense, standing wave patterns. In contrast, the CEOF patterns are based on a matrix of the co- and quadrature-spectra, and represent progressive wave patterns i.e. the modes may exhibit phase lags over the SST field. The OEOF's give spatial and temporal scales, with frequency dependence.

Recognizing that the processes affecting SST are sometimes seasonally dependent (e.g. runoff), some EOF analyses have been performed on seasonally-stratified data. Where seasonal averages have been used (e.g. 35 winter average SST's 1946 to 1980, for each of the twenty-four areas), the analysis is termed (N) analysis. Where the input series has consisted of monthly anomalies, 12 each year, the analysis is termed (N x 12). Where the input series has consisted of e.g. the three winter months for 1946 followed by the three winter months for 1947, as in

Jan 46, Feb 46, Mar 46, Jan 47, Feb 47, Mar 47, etc., the designation used is (N x 3).

We present (N), (N x 3) and (N x 12) EOF analyses of the 24 SST signals, based on the covariance matrix. Our results thus extend the (N) analysis of LT which was based on the correlation matrix. The shift to the covariance matrix is necessary in order to reconstruct the 'geophysical-scale' version of the SST field (termed the GSST field) - a step taken below. Using the covariance matrix, the input signals are in effect weighted by their respective variances prior to extraction of coherent patterns. The results are summarized in the tables of Appendix A.

RESULTS AND DISCUSSION

The Seasonal Cycle in SST's

The distributions of long-term averge SST's by month (base period, 1946-1980) are shown in Figures 3 a) to l). The contours trace the positions of the shelf/slope and slope/Gulf Stream fronts and are consistent with the corresponding charts in the U.S. Navy Marine Climate Atlas of the World (1981). (The contour scheme was chosen to include the seven degree isotherm which is associated with the vernal migration of mackerel (see Loucks, 1982)). The main features of the sequence are that the isotherms run approximately parallel to the topography, that there is a localized region of minimum SST off southwest Nova Scotia in summer, that the slope water region is one of maximum spatial gradient in SST, and that the on/offshore gradient is much stronger in winter than in summer. The latter point will be addressed again below.

Seasonal ranges of SST are low (7°C) in the south (Gulf Stream/Sargasso Sea) and in the north (Labrador Sea/Labrador Coast) and maximum (16°C) over

continental shelves off the northeastern United States and Nova Scotia. The seasonal range is intermediate (13-14°C) over the Grand Banks and around the Gulf of Maine.

Seasonal ranges are low in the Gulf Stream because of rapid advection of subtropical waters, with their thermal properties almost intact (seasonal cycles are minimal in the tropics). Seasonal ranges are reduced in the Labrador regions because of the lower limit at the freezing point. Seasonal ranges over the continental shelves are likely enhanced in response to seasonal shifts in wind patterns, and diminished by strong tidal mixing.

Given the average SST field by month, we shall now turn our attention to the departures from these averages - the monthly anomalies.

Monthly Anomalies in Comparison to Summer-Winter Differences

Comparisons in degrees Celsius were made between the range of the monthly anomalies and the range of the seasonal cycle in SST. The variance of deseasonalized, or (N x 12), monthly anomalies (Figure 4) is highest in the slope water region ($2.64°C^2$), lowest in the Sargasso ($0.36°C^2$), and intermediate over the continental shelves. Anomaly ranges (taken as four times the standard deviation) vary from 25% (Eastern Shore and Sable Island Bank) to 65% (Flemish Cap, Labrador Sea, Labrador Coast) of the seasonal range (the summer-winter difference) of SST (Table 1).

The high variance of anomalies in the slope water region is interpreted to be a result of the movement of the fronts in a region of strong spatial gradients and of the irregular occurrence of warm core eddies, cast off from the Gulf Stream and injecting heterogeneity i.e. anomalies. The anomaly variance is likely low in the Sargasso because it is distant from boundary areas of high gradients and strong

winds, and has a small seasonal temperature range. (An area with large seasonal range is vulnerable to large anomalies arising from slight shifts in timing of vernal warming or autumnal cooling). Over the continental shelves, the SST field is subject to the up/downwelling and heat flux influences of winds coming off the continent thermally unequilibrated to the sea, to the advective effects of coastal currents stimulated by river runoff and wind, and to incursions of slope water. Thus for the shelf area, the variance of anomalies is significant although not as large as in the slope water region.

Spatial Scales of the Anomaly Field

Trites et al. (1985) show the scale of regions of similar monthly anomalies of coastal SST's to extend over ∿ 1500 kms from Hamilton Bank (54 N; 54W) to Cape Sable (43.5N; 65.5W). In LT, OEOF (N) patterns are used as a gauge of SST spatial scale by season. The scale of the first mode, a generally uniform (positive or negative) anomaly reaches approximately 2500 ± 500 km (Cape Hatteras to Labrador). The pattern is centred on the Scotian Shelf in winter (January, Febraury, March). The centre shifts northeastward over the Grand Banks in spring (April, May & June), returns to the Scotian Shelf in summer (July, August, September), and moves southwestward to the New England shelf in autumn (October, November & December). The second mode is distinctive and robust to a variety of EOF analyses. It consists of peaks on the Grand Banks and on the Mid-Atlantic Bight, 180 degrees out of phase, with a node in the vicinity of the Gulf of Maine. The scale of a peak region is approximately 800 ± 200 km where the corresponding scale for the first mode is 2500 km. Superposition of the second mode on the first will reduce the apparent scale from 2500 km and is thus consistent with the sacle of ∿ 1500 km indicated in the coastal SST anomaly plots, reported by Trites et al. (1985), for the 1972-83 period.

The results of the (N x 3) seasonal analysis are shown in Figures 5 to 8; the figures show both the variances and the first mode EOF pattern coefficients, by season. In winter, the SST signals with highest variance are found in the East and West Slope Water areas (Figure 5). The winter (N x 3) first mode pattern is similar to that of autumn (see below) except that there is greater coherence between the shelf waters and the slope waters than in autumn. The scale is at least 1500 kms in the alongshore direction.

In spring (Figure 6), the variances are again largest in the slope water areas; however, the pattern of coherent variances of the first mode is centred shoreward of the slope water - extending some 2000 kms along the shelves from the mid-Atlantic Bight to the Grand Banks. The Labrador Sea and Cape Farewell areas do not respond in the first mode.

In summer (Figure 7) variance of SST in the slope water areas is diminished while variance on the Grand Banks is increased. Peaks in the first mode pattern seem concentrated around separate regions of high variance on the Scotian Shelf and the Grand Banks. One possibility is that the runoff freshet/estuarine current pulse, which is known to arrive at Cabot Strait in August, is responsible for the split pattern. In summer, the Labrador and Cape Farewell areas show some first mode coherence. This could be facilitated by the shallow seasonal thermocline; the effect of flux is confined to a shallow layer so that meteorological coherence can be more easily reproduced in SST coherence.

In autumn (Figure 8), the first mode has a scale of approximately 1500 kms and is shifted southwestward to a region of rather low variance between the South Shore and South New England areas, including the West Slope Water area.

In summary, the seasonal (N x 3) analyses show first mode length scales somewhat smaller than those from (N) analyses in LT - undoubtedly due to the

unequal weighting by variance in the former rather than the equal weighting for all areas implicit in the latter. Coherence betwe the slope water region and the shelf from Sable Island to the Mid-Atlantic Bight in winter is a feature of the (N x 3) analysis but not of the (N) anlaysis. Both analyses support the impression that, although the patterns shift with season, there exists (first mode) coherence alongshore from the Mid-Atlantic Bight to at least the Scotian Shelf, and in spring to the Grand Banks, and in summer to the Labrador Sea and Greenland.

The second mode in (N) and (N x 3) (not shown) exhibits a consistent modulation upon the basic pattern with strong responses on the Grand Banks and in the Mid-Atlantic Bight, out of phase, and with a node in the vicinity of the Gulf of Maine.

In summary, scales of $\curvearrowleft$ 1500 km observed from actual anomaly plots can be rationalized with scales of 2500 ± 500 km from EOF analysis; it would appear that there is a first mode with scale $\curvearrowleft$ 2500 km and that the superposition of the second mode (800 ± 200 km) reduces the scale of an EOF composite to $\curvearrowleft$ 1500 km consistent with observations.

Temporal Scales of the Anomaly Field

Temporal scales will be discussed first in terms of seasonal variances and then in terms of time series and power spectra. Finally the time (phase) lags resulting from complex empirical orthogonal function (CEOF) analysis will be presented.

Seasonal Variances

That anomaly variances exhibit a seasonal time scale is shown by the shifts in (N x 3) variances. The most marked shift is in the slope water areas where the

variances are large in winter (Figure 5) and spring (Figure 6) and quite small in summer (Figure 7) and autumn (Figure 8). These high variances are coincident with the occurrence of strongest temperature gradients between the Gulf Stream and shelf waters in winter and spring, and may, as well, be related to the wind fields; in summer, the on/offshore SST gradient is reduced as the seasonal thermocline becomes established, thus reducing the potential for large variance of anomalies. In contrast, variances over the Grand Banks, southern Scotian Shelf and Gulf of Maine are minimum in winter and maximum in summer. The minimum variance between winters in boreal waters may be caused by the lower limit on SST imposed by heat of fusion and the freezing point. The increased variance in spring compared to winter over these same shelf areas may arise through slight shifts in the timing of vernal warming; the strong temporal gradients in spring and autumn enhance the probability that anomalies will occur. The higher summer variance could be due to the greater sensitivity to meteorological effects resulting from the reduced mixed-layer depth.

Time Series

While time series of SST anomalies for individual areas are not illustrated, the monthly series for the first and second (N x 12) EOF modes are shown in Figure 9 (a) and (b). The first mode series is dominated by low frequency perturbations and shows the warm and cool periods centred around 1951 and 1965 respectively. The second mode series also shows some low frequency variability.

Spectra

Describing the set of SST power spectra (e.g. Figure 10), one can say that they are 'red' i.e. decreasing with frequency except in the Labrador region. In fact

for some of the areas (e.g. Central Grand Bank and Mid-Atlantic Bight), the spectra fit the power law, frequency to the power -1 implying that they are not integrable i.e. variance grows with the length of the time series. Therefore, we must specify that the spectra describe the energy between periods of 35 years and 2 months.

From a power spectrum of the SST anomalies, one can define the half-power period as that period at which the power is divided into two equal portions - one at larger time scales and one at smaller. Half-power periods or median time scales from the (N x 12) power spectra are shown in Figure 11. They range from 6 months on the Labrador Shelf to 28 months in the Gulf of Maine. In fact, the highest median time scales are found for the coastal region from the Gulf of Maine to the Mid-Atlantic Bight. If the SST anomaly spectra were white, the half-power period in these analyses would be 4 months (twice the folding period). Although the wind spectra are white (Appendix B), the SST spectra are weighted more toward the low frequencies. One challenge is to suggest why this should be.

A note of caution must be sounded: in a few cases, e.g. Gulf of St. Lawrence, St. Pierre Bank, Labrador Coast, Cape Farewell, data for some months are extremely sparse or non-existent. Where data are sparse and the variance is very large, interpolated values have been substituted; where data are missing, the long term average median for the month has been substituted. Sparse data and substituted averages tend to inject high frequency variance and so lead to median time scales biased toward shorter times. This may be occurring to some extent in the aforementioned areas, although the substitutions of data were very few. It is likely that median time scales over the Labrador Shelf, Cape Farewell, Saint Pierre and the Gulf of St. Lawrence areas really are relatively short, perhaps because ice-cover insulates the water-column from the winter air-sea exchanges which are strong in other areas.

In the Western Slope Water area, the half-power period is 17 months for the SST's. Smith and Petrie (1982) assessed the time scale of the movement of the shelf/slope front in this area. In their 3-year analysis, the folding period was 2 weeks; most of the energy of the first EOF mode was concentrated at periods from 6 months to a year. These two results are interpreted as being consistent insofar as they are comparable. (The 35-year span of this SST analysis would be expected to incorporate more low-frequency information).

As in Smith and Petrie (1982) we have calculated the half-power period for the mode series. For the first mode, whose spatial scale is about 2500 kms, the median time scale is 34 months. For the 800 km second mode, the median time scale is 29 months. These results serve to emphasize the difference between the meteorological forcing (e.g. the wind with median time scale of 6 months) and the oceanic response. The long ocean time scales may arise through the fact that the ocean responds more strongly (i.e. baroclinically) to low frequency forcing, or through thermal inertia, or effects of runoff where the half-power time scale is 43 months (Appendix C), or through subsequent reinforcement by surface fluxes.

The total variance in the SST field for all areas combined is partitioned 17% in the (half-width) 'zero' frequency band, 24% in the 24-month band, 13% in the 12-month band, 9% in the 8-month band, 7% in the 6-month band, etc. so that 70% of the variance (given the folding period of 2 months) occurs at time scales of 6 months or greater, and with a peak at low frequency.

SST spectra for five selected areas are shown in Figures 10 (a) to (e) together with plots of coherence and phase. Coherences tend to reach significant levels only for low frequencies. There are 88 degrees of freedom; the 95% confidence level factors are 0.7 and 1.3 for the power spectra, and 0.25 for coherence. The power spectra do not differ significantly.

Figure 10(d) compares Western Slope Water and mid-Atlantic Bight (MAB) area. Coherence is high at low frequencies. Phase shows a progression: WSL leads MAB linearly with increasing frequency - the signature of advection - with a lag of about 1.5 months.

Figure 10(e) compares the mid-Atlantic Bight and Central Grand Bank areas. Coherence is relatively high at low frequencies. Phase lag is 180 degrees for frequencies up to 1/(12 months) where the coherence is high.

It is at first curious that phase lags are all small at lowest frequencies except for CGB and MAB (Figure 4 e) where there is 180 degrees phase difference. It would seem that for neighbouring areas (as in Figures 10 a to d) first mode patterns appear in the cross-spectra whereas for the separate areas CGB and MAB (Figure 10 e) the second mode, in which the signal-to-noise ratio increases with separating distance, appears in the cross-spectra.

CEOF's

The spectra were also used to compute the complex EOF modes of the SST feild. The COEF's admit progressive wave patterns whereas the OEOF's are restricted to standing wave modes. Nevertheless, the CEOF's show first and second modes (Figures 12 and 13) consistent with those of the OEOF analysis above. The first mode for the 12-month band (Figure 12) suggests an advective or progressive wave component, propagating from north to south with phase lag approximately 100 degrees or 3 months between Labrador and the mid-Atlantic Bight.

There are potential problems with using CEOF's to identify advective patterns in this case. If direct meteorological forcing occurs with zero lag and the runoff effect occurs with a lag of several months, the CEOF analyses may respond

to the composite cross-spectra and show lags which are less than those expected. One tactic for circumventing this would be to first adjust the SST's by removing the wind effect and then recompute the CEOF's in the expectation that the runoff effect may emerge clearly. We plan to do this in future studies.

As an aside, a CEOF analysis was carried out on the offshore component of geostrophic winds (Thompson and Hazen, 1983) for the mid-Atlantic Bight, Gulf of Maine, Scotian Shelf, and Grand Banks. The most striking result was that the winds exhibited a second mode comparable to that of the SST's i.e. with strong responses over the Grand Banks and the mid-Atlantic Bight, 180 degrees out of phase. This suggests that the SST second mode may arise from the winds' second mode.

Summary

Although changes certainly occur on a seasonal scale (3 months), the median time scale for SST anomalies is 6 to 30 months. The power spectra show energy and coherence concentrated in the low frequency bands, with component signals either almost in-phase or 180 degrees out-of-phase. The relatively large half-power periods for the first and second modal series, 34 and 29 months respectively, again reflect the fact that coherence between areas is concentrated in the low frequency bands. These dominant mode SST time scales are intermediate between those of the runoff (RIVSUM, 43 months) and those of the wind (approximately 4 months), as are the median time scales of the individual SST areas. (Of course, the first and second modes for the winds may also prove to have median time scales larger than the wind signals themselves; this information is not yet available.) In any case, the evidence is that the strongest modes are describing large-scale, relatively low-frequency, standing patterns. The question remains: how can this low frequency coherence arise (directly and indirectly) from a "white"

meteorological driver? The periods involved are too long to arise simply from thermal inertia; one would not expect thermal inertia effects to extend beyond one year unless there was persistent meteorological reinforcement.

RECONSTRUCTION OF THE SST FIELDS FROM EOF MODES

Reconstruction Technique

A feature of the EOF analysis, beyond identification of spatial scales from the mode shapes and time scales from the power spectra of the mode series, is the opportunity of reconstructing the 24-area SST field using, for example, just the six most significant modes (Haney et al., 1983). A spatial smoothing is thereby achieved, allowing contouring. The GSST approach for smoothing an oceanographic or meteorological scalar field has advantages over, for example, Objective Analysis. In the case of the latter, it is necessary to specify the drop-off of the correlation in the directions of neighbouring areas. This becomes complicated when the field of interest encompasses several different regimes such as shelf waters, deep ocean, the Gulf Stream, etc. With the GSST approach, the spatial smoothing occurs on the basis of regional (as distinct from area-to-area) covariance.

Figure 14 shows a plot of the eigenvalues for the (N x 12) analysis: the trend line indicates the progression of eigenvalues resulting from the analysis of random noise; the falloff for the highest mode numbers reflects the finite length of the data series; the first and second eigenvalues, and even the third through sixth, lie above the trend of the noise and are considered significant (Preisendorfer & Barnett, 1977). Therefore the SST field will be reconstructed utilizing the first six modes only. Haney et al. (1983) term as "geophysical scale" the fields reconstructed from the EOF modes. We shall use the abbreviation, GSST, for the

geophysical-scale SST field reconstructed by convolving the modal co-efficients of the significant modes for the particular area of interest with the respective modal time series.

Before presenting the GSST's, an error analysis of the GSST process (Table 1) will be discussed. The table consists of five columns of results. The seasonal range, August minus March SST, and the (N x 12) variance are shown in the first and second columns. The third column shows the variance "explained" using the six mode reconstruction. This is calculated by convolving the significant eigenvalues with the square of the eigenvector coefficients (the loadings) for the particular area. The fourth to sixth columns contain three expressions of the "unexplained" variance and standard deviation. The seventh column shows the standard error of the monthly median, calculated as the root of ($\pi/2$ x variance/number of observations). Table 1 reveals that: (1) This analysis, based on the co-variance matrix, gives emphasis to those areas with greatest variance; the explained variance is some 90% of the total for the slope water areas whereas 60 to 70% of (a smaller) total variance is explained on the continental shelves. (2) The standard deviation of the unexplained portion of the SST signal exceeds the within-month uncertainty. This is proper, otherwise the EOF analysis would be pushed beyond the intrinsic precision of the data base. (3) The Labrador Coast, Labrador Sea, Cape Farewell, and Sargasso Sea regions show high percentages of unexplained variance and will be poorly reproduced in the GSST version because of low spatial coherence. Table 2 compares the GSST's with the monthly median SST's. The GSST's are smoothed regionally by definition; this has the effect of smoothing their time series as well. The differences in Table 2 correspond to the unexplained variances in Table 1.

Having determined the significant eigenvectors and calculated the errors associated with the GSST field, we proceed to present February and August GSST charts for 1950-1952, and then the monthly charts for 1951 - from the EOF's, a year of extreme positive anomalies. The corresponding charts are then presented for 1965, a year of extreme negative anomalies, and for February and August of the adjoining years to check the longer term persistence of the anomalies. Later, a brief account is given of a mostly unsuccessful attempt to use the GSST's to isolate the runoff effect, an exercise that is instructive regarding the questions which can and cannot appropriately be asked using the EOF technique.

Results on a Yearly Time Scale, 1950-52 and 1964-66

From the EOF mode series, 1951 was a year of extremely high mode 1 anomalies and 1965, a year of extremely low mode 1 anomalies. In this section, a scan is made of the three-year period around the extreme to see if longer-term persistence is evident.

Figure 15 (a) shows the GSST anomalies to have been negative east of the Scotian Shelf and positive on the Scotian and New England Shelves in February 1950. (There are exceptions, all minor except in the Labrador Sea and Cape Farewell areas. However, these areas are, by Table 1, known to be poorly reproduced.) Figure 15 (b) shows that during this season, winds were offshore in the former area and onshore in the latter area. The interpretation made is that wind effects on SST are strongly dependent on wind direction: sensible heat fluxes are dependent on wind direction because winter (air-sea) temperature differences tend to be negative for offshore winds from the continent and positive for onshore winds from the Sargasso; latent heat fluxes (identified as the major source of variation in net heat exchange by Bunker and Worthington, 1976) will exhibit this

dependence because of the shift in surface air stability; advective effects are dependent on wind direction because offshore anomaly winds drive upwelling of cold intermediate layer waters and shift the shelf/slope front offshore while onshore anomaly winds mean the actual winds are light.

In August, 1950, (Figure 16) the region of negative GSST anomaly had shifted a few hundred kilometres westward; winds were light. By winter, 1951, (Figure 17 a) the region of positive GSST anomalies was widespread, oriented on/offshore, with a ridge of maximum anomalies leading from the Eastern Slope Water area to the LaHave Bank area. Consistent with this, the wind stress was directed onshore between Cape Hatteras and the Grand Banks (Figure 17 b). Figure 18, for summer, 1951, but representative of summer conditions generally, shows summer anomaly winds to have been very light and GSST anomalies to resemble those of the winter distribution. Figure 19 (a), for winter, 1952, shows GSST's rather similar to those of winter, 1951. The wind stress was again directed onshore alhtough the magnitudes were reduced compared to 1951. Figure 19 (b), for August, 1952, shows GSST's fairly similar to those of the previous February.

There appears to be persistence across several years of anomaly wind stress direction in winter, leading to consistent GSST patterns exhibiting widespread positive anomalies. Let us now see if this persistence exists during a period of extreme negative anomalies.

In winter, 1964, an anomalously low pressure area was centered at 50N, 45W (Thompson and Hazen, 1983). The circulation around this low resulted in offshore winds from the Grand Banks to the mid-Atlantic Bight. Figure 20 (a) shows negative GSST anomalies for February, 1964. Anomaly winds were light over the western North Atlantic in spring and summer; the GSST distribution for August, 1964, (Figure 20 b) is comparable to that for the previous February. In winter,

1965, the wind stress (Figure 21) was again directed offshore for the Scotian Shelf and the New England Shelf, but onshore for the Grand Banks. The GSST's show negative anomalies in the offshore air flow and positive anomalies in the onshore air flow. Figure 22, for summer, 1965, further illustrates that summer wind anomalies are small, in contrast to the winter situation, whereas summer GSST patterns are similar to those of winter. In winter, 1966, anomaly windstress (Figure 23) was strong and directed offshore west of Cape Race, Newfoundland. The GSST's were preponderantly negative in this region. In the eastern region, with onshore winds, GSST's were positive. Spring and summer anomaly winds were light in 1966; the August GSST pattern (Figure 24) is again similar to that for the previous February.

In summary, winter wind anomalies, onshore or offshore, appear to repeat between years over the eastern seaboard, particularly west of Newfoundland, at least during episodes of extreme SST anomalies. It may be that such persistence in winds is a prerequisite for extreme SST's; this merits further study. Summer anomaly wind stresses appear negligible. GSST anomalies appear to vary in response to the direction of the strong (e.g. winter) wind anomalies. Unlike the winds, winter GSST anomaly patterns persist into summer. The possible pathways for such persistence to arise are considered later.

Results on a Scale of Months, 1951 and 1965

GSST's for the period, January to April, 1951 (Figures 17 and 25) show quite consistent distribution. Temperature anomalies are potentially highly variable during the May-July period because of shifts in the timing of vernal warming. Some such shift in timing may explain why June 1951 (Figure 25) anomalies appear to have decreased compared to those of April and August, where the patterns and

magnitudes are quite similar. This sensitivity to timing exists again in autumn; thus a slightly early onset of autumn cooling may account for the decresed anomalies (constructed and observed) in October, 1951. Correspondingly, the slope water areas, being areas of strong spatial gradients, are sensitive to geographical shifts in fronts, as may have occurred in May, 1951 (Figure 25). Beyond these special cases, the overall impression gained from the series of monthly GSST charts through 1951 is that the GSST pattern evolves very slowly during the year of extreme positive anomaly.

The GSST charts for January to April, 1965, (Figures 21 and 26) show a slow migration of the zero contour from northeast to southwest. This progression is apparently disrupted in May and June (Figure 26), perhaps by a slight delay in warming, but reappears, having progressed southwestward, in August (Figure 22). Through the autumn of 1965 (Figure 26), the distribution of GSST anomalies remains practically constant. The anomaly wind stress fields are negligible during the latter half of 1965. This is also a year of very low river runoff. The negative SST anomalies may simply be reflecting the dearth of runoff and concomitant stratification. It is curious, nevertheless, that the SST anomalies should suggest the shelf/slope front to be further offshore than usual when the transport of the Nova Scotia Current is inferred to be less than usual. The resolution to this puzzle lies, we suggest, in the synchronicity between runoff and offshore effects as linked by meteorological forcing. Again for an extremely cool year as for an extremely warm year, the GSST pattern evolves very slowly.

The overall impression conveyed from examining these GSST chart series is that along this seaboard winter winds show between-year persistence, the winter SST's respond to the anomaly wind stress field - positive GSST anomalies are associated with onshore anomaly winds and negative GSST anomalies, with offshore

anomaly winter winds - and summer GSST anomalies persist in winter patterns even through winter wind patterns do not survive into summer. (However, winter wind effects seem to be reinforced by summer cloud patterns.) A possible explanation of this is that the winter winds, through transfers of sensible and latent heat, condition the heat content of the mixed water column and that this conditioning persists and, reinforced by the cloud cover anomaly and runoff effects, influences summer SST's through all the heat budget processes.

HYPOTHESIS

Two main themes emerge. In the SST field, space-scales are large - on the order of 2500 kms - and time scales are long - longer than those of the wind field. One can offer a two-part hypothesis to interpret these results.

The large spatial scales of SST seem to arise with and correspond to those of winter winds with their associated sensible and latent heat fluxes and perturbations of advection. The GSST chart series support the relationship of winter SST patterns and winter anomaly winds, both in terms of spatial scale and direction - whether onshore (warm SST) or offshore (cool SST). To suggest why these winter SST patterns should persist through subsequent seasons i.e. exhibit long time scales is more difficult; there are several possibilities including thermal inertia and baroclinic response preferentially at low frequencies. Keying on the evidence in LT that there is a correlation peak between winter and summer SST's, it is suggested that the long time scales arise because of reinforcement of winter anomalies in summer and autumn.

Summer surface heat flux anomalies might be examined to see if they serve to reinforce those of winter i.e. to see if they are correlated. Preliminary examination of cloud data suggests they do reinforce.

Autumn reinforcement of winter anomalies can arise through runoff. For examle, high/low spring runoff from St. Lawwrence rivers is correlated with onshore/offshore anomaly winds on the Scotian Shelf in winter (Koslow et al., 1985). Autumn SST's on the Scotian Shelf show the reinforcing influence of this runoff.

CONCLUSIONS

SST anomaly ranges (taken as four times their standard deviation) are on the order of 4 Celsius degrees and are 25% to 65% of seasonal SST ranges. Anomaly ranges are largest in the slope water region, because of the large spatial gradients there (especially in winter), and smallest in the Sargasso Sea.

The (N x 12) variance of SST is concentrated in the slope water region for time scales 2 months and longer - reflecting the strong spatial gradients of SST there. However, the regions of greatest (N x 3) variance shift markedly with season. (The wind and particularly the river runoff also show strong seasonality.)

The dominant spatial scale of SST patterns is large (2000 to 2500 km) in the longshore direction, from at least Cape Hatteras to Flemish Cap, and smaller (200 km) in the on/offshore direction. This longshore scale, revealed by EOF analysis, is larger than scrutiny of actual data would suggest; superposition of the first (2500 km) and second (800 km) EOF modes reduces the composite scale to the 1500 kms observed.

The EOF technique emphasizes the dominant patterns. These dominant patterns show remarkable persistence from season to season. Although the centre of the first mode pattern shifts northeast in spring and southwest in autumn, the character of the mode remains relatively unchanged. This is surprising in view of the seasonality of the wind and runoff. For example, charts of geostrophic winds (Thompson and Hazen, 1983) are entirely different, winter to summer.

The SST power spectra show power concentrated in the low frequencies, some evidence of northeast-to-southwest advection, and responses on the Grand Banks and in the mid-Atlantic Bight which are 180 degrees out-of-phase - i.e. second mode behaviour.

Half-power periods or median time scales for the individual SST areas range (given the folding period of two months) from approximately 6 months to 28 months. However, the corresponding values for the time series of the first and second SST (N x 12) modes are 34 and 29 months respectively. The dominant SST modes describe large-scale, relatively low-frequency, almost standing patterns. Their time scales are intermediate between those of the winds (approximately 6 months) and the runoff (43 months). The shift in time scales between winds and SST may be partly due to the time scale of runoff and partly due to the fact that the ocean shows strongest (i.e. baroclinic) response to low-frequency forcing.

The CEOF analysis generally confirmed the uniform first mode and "tilting" second mode patterns. However, the advection of 'wave' modes through the field may have been obscured by the superposition of wind and runoff effects in the covariances and spectra.

Preliminary computations connect the second SST mode with the occurrence of a comparable mode in the atmospheric pressure field.

The EOF approach is used on both a seasonal and a deseasonalized basis. The deseasonalized analysis supports computation of spectra with the advantage that the range of time-scales can be quantified and with the disadvantage that seasonal events are averaged over. The seasonal analyses ((N) and (N x 3)) preserve the character of seasonal events and provide a glimpse of the complex organization of the atmosphere/ocean system. For example, large-scale meteorological patterns in winter appear to set up effects in spring, summer and autumn, which reinforce and prolong the winter SST anomalies.

The EOF technique is not well suited to detecting and enhancing a secondary, related (non-orthogonal) effect such as the river advective effect.

The GSST fields, being spatially smoothed, are easier to interpret than the SST fields in terms of atmospheric pressure, winds, runoff, etc. They can readily be generated for any year in the period 1946-1980. There is also potential for predicting GSST fields several months in advance based on, for example, Box and Jenkins (1970) forecasts of the six ingredient EOF modal series; the eigenvector coefficients already determined would be convolved with the projected modal series. With respect to the interpretation of the GSST fields for the extreme years, 1951 and 1965, there are three points to be made: The GSST charts exhibit much more persistence between years than do the wind stress charts, although persistence is recognizable in them too; the latter may be a pre-requisite for extreme SST years. This is identified as a point deserving further study. The GSST charts evolve slowly within the year while the wind charts tend to show anomaly fields much stronger in winter than in summer. The GSST fields appear to respond to the direction (and strength) with warm temperatures in a period of onshore anomaly winds (e.g. 1951) and cool temperatures in a period of offshore anomaly winds (e.g. 1965).

The GSST signals for the Offshore Labrador Current and West Grand Bank areas correlate rather strongly with onshore winds in winter and spring, but not in summer and autumn. Noting that, for these two areas as for others, 1951 was a year of strong positive anomalies and 1965, a year of strong negative anomalies in summer and autumn as well as winter and spring, these results support the hypothesis that the persistence of anomalies and of EOF patterns among them is associated with forcing mechanisms which are correlated, lagged and reinforcing.

The hypothesis concerning the relatively large geographic and temporal scales is that the space scales arise through the effects of large winter meteorological anomaly patterns, and the time scales arise from summer and autumn reinforcing of winter anomalies through, for example, correlated summer cloud cover and runoff.

ACKNOWLEDGEMENTS

We thank our colleague, J.A. Koslow, who has provided Figure 9 and partaken in discussions of this work throughout.

REFERENCES

Bunker, A.R., and L.V. Worthington. 1976. Energy exhcnage charts of the North Atlantic Ocean. Bull. Amer. Meteor. Soc., vol. 57, No. 6, 670-678.

Davis, C.W. 1978. Seasonal bottom-water temperature trends in the Gulf of Maine and on Georges Bank, 1963-75. NOAA Technical Report NMFS SSRF-725. 17 p.

Haney, R.L., B.H. Hautman, and W.H. Little. 1983. The relationship between wind and sea surface temperature anomalies in the mid-latitude North Pacific Ocean. J. Phys. Oceanog. Vol. 21(2), 168-186.

Koslow, J.A., R. Loucks, K.R. Thompson, and R. Trites. In press. Relationships of St. Lawrence River outflow with sea-surface temperature and salinity in the Northwest Atlantic. In The role of freshwater outflow in coastal marine ecosystems. NATO Symposium volume, Springer-Verlag.

Loucks, R.H. 1982. Analysis of the feasibility of forecasting the vernal progression of isotherms along the Atlantic coast of Nova Scotia. Manuscript report submitted to Marine Ecology Lab., Bedford Institute.

Loucks, R.H., and R.W. Trites. 1985. Analyses of sea-surface temperatures in the Northwest Atlantic. Can. Tech. Report of Fish. Aquat. Sci. No. 1410: iv + 42 pp.

Preisdendorfer, R.W., and T.P. Barnett. 1977. Significance tests for empirical orthogonal functions. Reprints, Fifth Conf. Probability and Statistics in Atmospheric Sciences, 15-18 Nov. 1977. Las Vegas, Am. Meteorol. Soc., p 19-172.

Robinson, A.R. 1971. The Gulf Stream. Phil. Trans. Roy. Soc. A, 270, 351-370.

Smith, P.C., and B.D. Petrie. 1982. Low-frequency circulation at the edge of the Scotian Shelf. J. Phys. Oceanogr. Vol. 12, 28-46.

Smith, S.D., and F.W. Dobson. 1984. The heat budget at Ocean Weather Station Bravo. Atmosphere-Ocean, 22(1), 1-22.

Thompson, K.R., and M.G. Hazen. 1983. Interseasonal changes of wind stress and Ekman upwelling: North Atlantic, 1950-1980. Can. Tech. Rept. Fish. Aquat. Sci. No. 1214.

Trites, R.W., D.P. McLain, and M.C. Ingham. 1985. Sea-surface temperatures along the continental shelf - Hamilton Bank to Cape Hatteras. NAFO Studies 8: 21-23.

Trites, R.W., and R.H. Loucks. 1985. Environment on the East Coast and in particular the Scotian Shelf. In Proceedings of the Workshop of the Marine Environment and Ecosystem Subcommittee of CAFSAC, 30 Oct - 1 Nov. 1984, R. Mahon (ed.). Can. Tech. Rept. Fish. Aquat. Sci., No. 1347.

Sutcliffe, W.H.Jr., R. H. Loucks, and K.F. Drinkwater. 1976. Coastal circulation and physical oceanography of the Scotian Shelf and the Gulf of Maine. J. Fish. Res. Bd. Can. 33: 98-115.

U.S. Navy Marine Climatic Atlas of the World. 1981. Vol. IX, Supt. of Docs., U.S. Gov. Printing Office, Washington, D.C., 20402.

Table 1. Comparison of uncertainty remaining after GSST reconstruction with uncertainty inherent due to scatter in observations (N x 12). For each area the seasonal range is shown in Column 1, the total variance is shown in column 2, the variance 'explained' using 6 eigenvectors, in column 3, the remaining 'unexplained' variance of column 4 (calculated as col. 2 - col. 3) and expressed (column 6), and finally, for comparison, the standard error of the monthly median.

SST Area	August-March SST	(N x 12) variance	'Explained' variance	'Unexplained' var.	%	s.d.	Average Standard Error of monthly median
	C°	$(C°)^2$	$(C°)^2$	$(C°)^2$		C°	C°
ESS	16.8	1.09	0.66	.43	39	.66	.32
BR	12.8	1.72	0.93	.79	46	.89	.50
SS	15.2	1.69	1.19	.50	30	.71	.40
SI	15.6	1.09	.72	.37	34	.61	.26
LCS	6.6	1.40	0.46	.94	67	.97	.35
LS	6.8	0.96	0.29	.67	70	.82	.31
GB	12.3	1.37	0.86	.51	37	.71	.38
GOM	13.0	1.46	0.84	.62	42	.79	.29
SP	15.4	1.45	0.84	.61	42	.78	.51
OLC	11.5	1.95	1.16	.79	41	.89	.33
WGB	14.3	1.10	0.75	.35	32	.59	.22
ILC	13.0	1.22	0.85	.37	30	.61	.26
CGB	13.4	1.59	1.15	.44	28	.66	.30
FC	9.3	1.81	1.07	.74	41	.86	.60
ESL	11.2	2.27	2.17	.10	4	.32	.27
WSL	12.7	2.63	2.55	.08	3	.28	.29
SNE	16.4	1.94	1.54	.40	21	.63	.26
MAB	15.9	1.61	1.08	.53	33	.73	.15
GS	7.4	0.92	0.43	.49	53	.70	.23
SA	8.4	0.36	0.04	.32	89	.57	.13
GSL	16.2	1.87	1.45	.42	22	.65	.45
CFR	4.2	1.17	0.27	.90	77	.95	.43
Y	10.3	1.98	1.23	.75	38	.87	.44
LHB	14.9	1.76	1.14	.62	35	.79	.46

TABLE 2 COMPARISON OF MONTHLY MEDIAN OBSERVED ANOMALIES OF SST AND RECONSTRUCTED GSST FOR SELECTED AREAS DURING EXTREMELY WARM (1950-52) AND COOL (1964-66) YEARS

Extreme Warm		1950		1951											1952	
		Feb	Aug	Jan	Feb	Mar	Apr	May	Jun	Jul	Aug	Sep	Oct	Nov	Dec	Feb	Aug
CGB	GSST	-0.9	-1.0	1.2	0.8	0.7	1.7	0.6	1.5	1.8	2.1	1.1	0.7	0.9	0.7	0.9	3.6
	Actual	-0.2	-1.4	1.5	0.9	0.9	1.5	0.6	1.3	1.5	3.1	2.4	0.6	1.0	1.5	1.5	3.6
	Residue	-0.7	0.4	-0.3	-0.1	-0.2	0.2	0	0.2	0.3	-1.0	-1.3	0.1	-0.1	-0.8	-0.6	0
GSL	GSST	-0.2	0.1	1.1	-0.2	4.2	2.5	0.8	1.5	0.3	0.8	1.3	-0.1	0.1	1.0	0.1	2.6
	Actual	(.0)	-0.4	(.0)	0.1	5.8	2.3	0.7	1.3	-1.6	0.7	0.6	-0.5	-0.1	1.0	0.1	2.9
	Residue	-0.2	0.3	1.1	0.3	-1.6	0.2	0.1	0.2	1.9	0.1	0.7	0.4	0.2	0	0	-0.3
ESS	GSST	0.1	-0.3	2.3	1.9	2.4	2.5	1.4	1.4	1.8	2.1	2.1	0.5	1.2	1.2	1.5	2.8
	Actual	0.1	-1.2	3.2	1.7	1.7	2.5	1.1	0.3	2.4	1.0	1.8	1.1	1.1	1.5	2.8	1.5
	Residue	0	0.9	-0.9	0.2	0.7	0	0.3	1.1	-0.7	1.1	0.3	-0.6	0.1	-0.3	-1.3	1.3
GB	GSST	1.1	0.1	2.4	2.6	2.1	2.2	2.3	1.0	1.7	1.9	2.1	0.7	1.6	1.5	2.0	1.8
	Actual	1.9	2.1	1.7	1.9	2.2	1.9	3.6	1.3	2.0	1.5	.4	1.4	2.1	2.3	1.9	1.0
	Residue	-0.8	-2.0	0.7	0.7	-0.1	0.3	-1.3	-0.3	-0.3	0.4	-1.3	-0.7	-0.5	-0.8	0.1	0.8
WSL	GSST	-0.2	-0.2	1.8	1.5	2.1	2.5	4.3	1.4	0.6	1.3	0.6	0.8	2.3	2.3	1.6	1.3
	Actual	-0.4	-0.4	2.0	1.2	1.8	2.6	4.1	1.3	0.9	1.3	0.5	0.6	2.3	2.2	1.8	1.3
	Residue	0.2	0.2	-0.2	0.3	0.3	-0.1	0.2	0.1	-0.3	0	0.1	0.2	0	0.1	-0.2	0
GS	GSST	1.0	0.8	0.2	0.8	0.6	0.3	0.7	0.2	0.4	0.1	0.8	0.7	0.4	0.6	0.4	0.5
	Actual	2.3	-0.1	0.4	0.1	1.2	0	0.3	-0.6	0	0.5	0.6	0.6	0	0	1.2	1.0
	Residue	-1.3	0.9	-0.2	0.7	-0.6	0.3	0.4	0.8	0.4	-0.4	0.2	0.1	0.4	0.6	-0.8	-0.5
MAB	GSST	2.5	0.8	0.8	1.7	1.5	1.1	1.8	0.3	0.9	0.7	1.6	0.9	1.0	1.2	1.2	0.9
	Actual	3.5	0.9	1.0	2.4	1.3	1.8	1.6	-0.1	-0.1	0.4	0.8	0.4	0.9	1.1	1.3	0.4
	Residue	-1.0	-0.1	-0.2	-0.7	0.2	-0.7	0.2	0.4	1.0	0.3	0.8	0.5	0.1	0.1	-0.1	0.5

Cool Years		1964		1965											1966	
		Feb	Aug	Jan	Feb	Mar	Apr	May	Jun	Jul	Aug	Sep	Oct	Nov	Dec	Feb	Aug
CGB	GSST	-0.1	-0.2	-0.3	0.2	0.3	0.4	-0.7	-1.0	-1.1	0.5	0.6	-0.1	-0.6	0	0.9	1.4
	Actual	-0.2	-0.1	-0.4	-0.2	-0.2	0.2	-0.3	0.2	-0.3	-0.2	-0.5	-0.1	-0.3	0	0.4	1.1
	Residue	0.1	-0.1	0.1	0.4	0.5	0.2	-0.4	-1.2	-0.8	0.7	1.1	0	-0.3	0	0.5	0.3
GSL	GSST	0.1	0.2	0	0.6	-0.1	0.4	0	1.4	-0.1	-5.3	-2.9	-3.1	-1.0	-0.5	0.6	-0.8
	Actual	0.2	0.7	0.8	1.2	-0.2	-0.5	-0.4	2.9	0.2	-6.9	-2.7	-4.0	-0.1	-0.3	0.2	-1.3
	Residue	-0.1	-0.5	-0.8	-0.6	0.1	0.9	0.4	-1.5	-0.3	1.6	-0.2	0.9	-0.9	-0.2	0.4	0.5
ESS	GSST	-0.5	-1.4	-0.6	-0.4	-0.6	-0.8	-1.7	-1.4	-1.7	-1.8	-1.1	-1.4	-1.2	-0.9	0	-0.3
	Actual	-0.5	-1.8	-0.7	-0.4	0	-0.5	-1.8	-1.7	-1.6	-0.8	-0.9	-1.4	-1.1	-1.4	-0.8	-0.1
	Residue	0	-0.4	0.1	0	-0.6	-0.3	0.1	0.3	-0.1	-1.0	-0.2	0	-0.1	0.5	0.8	-0.2
GB	GSST	-1.4	-2.2	-1.7	-1.5	-1.1	-1.6	-1.4	-2.0	-1.9	-1.2	-1.3	-1.5	-1.7	-1.5	-1.9	-0.9
	Actual	-0.8	-1.8	-1.1	-1.5	-1.7	-2.3	-2.5	-1.9	-1.2	-1.2	-1.7	-1.3	-1.8	-1.8	-1.8	-0.8
	Residue	-0.6	-0.4	-0.6	0	0.6	0.7	1.1	-0.1	-0.7	0	0.4	-0.2	0.1	0.3	-0.1	-0.1
WSL	GSST	-3.6	-2.4	-4.9	-3.1	-0.2	0	2.8	0	-0.5	-1.2	-1.6	-2.6	-2.2	-1.6	-6.1	-0.8
	Actual	-3.8	-2.6	-5.0	-3.2	-0.1	0.4	3.0	-0.2	-0.7	-0.6	-1.7	-2.7	-2.1	-1.6	-6.1	-0.8
	Residue	0.2	0.2	0.1	0.1	-0.1	-0.4	-0.2	0.2	0.2	-0.6	0.1	0.1	-0.1	0	0	0
GS	GSST	-0.6	-0.5	-0.2	-0.6	-0.5	-0.6	-0.4	-0.7	-0.2	0.4	-0.5	-0.2	-0.5	-0.5	-0.3	-0.2
	Actual	-2.3	-0.6	-0.1	-1.0	-1.3	-1.1	-0.2	-0.6	-0.6	-0.3	-0.2	0	0.6	0.5	-0.9	-0.6
	Residue	1.7	0.1	-0.1	0.4	0.8	0.5	-0.2	-0.1	0.4	0.7	-0.3	-0.2	-1.1	-1.0	0.6	0.4
MAB	GSST	-1.1	-1.5	-1.0	-1.5	-1.1	-1.6	-0.8	-1.4	-1.1	-0.9	-1.5	-1.3	-1.5	-1.5	-1.4	-0.7
	Actual	-0.9	-0.7	-1.2	-1.9	-1.6	-2.1	-0.6	-1.2	-0.1	0	-0.3	-0.7	-0.8	-1.1	-2.0	-0.2
	Residue	-0.2	-0.8	0.2	0.4	0.5	0.5	-0.2	-0.2	-1.0	-0.9	-1.2	-0.6	-0.7	-0.4	0.6	-0.5

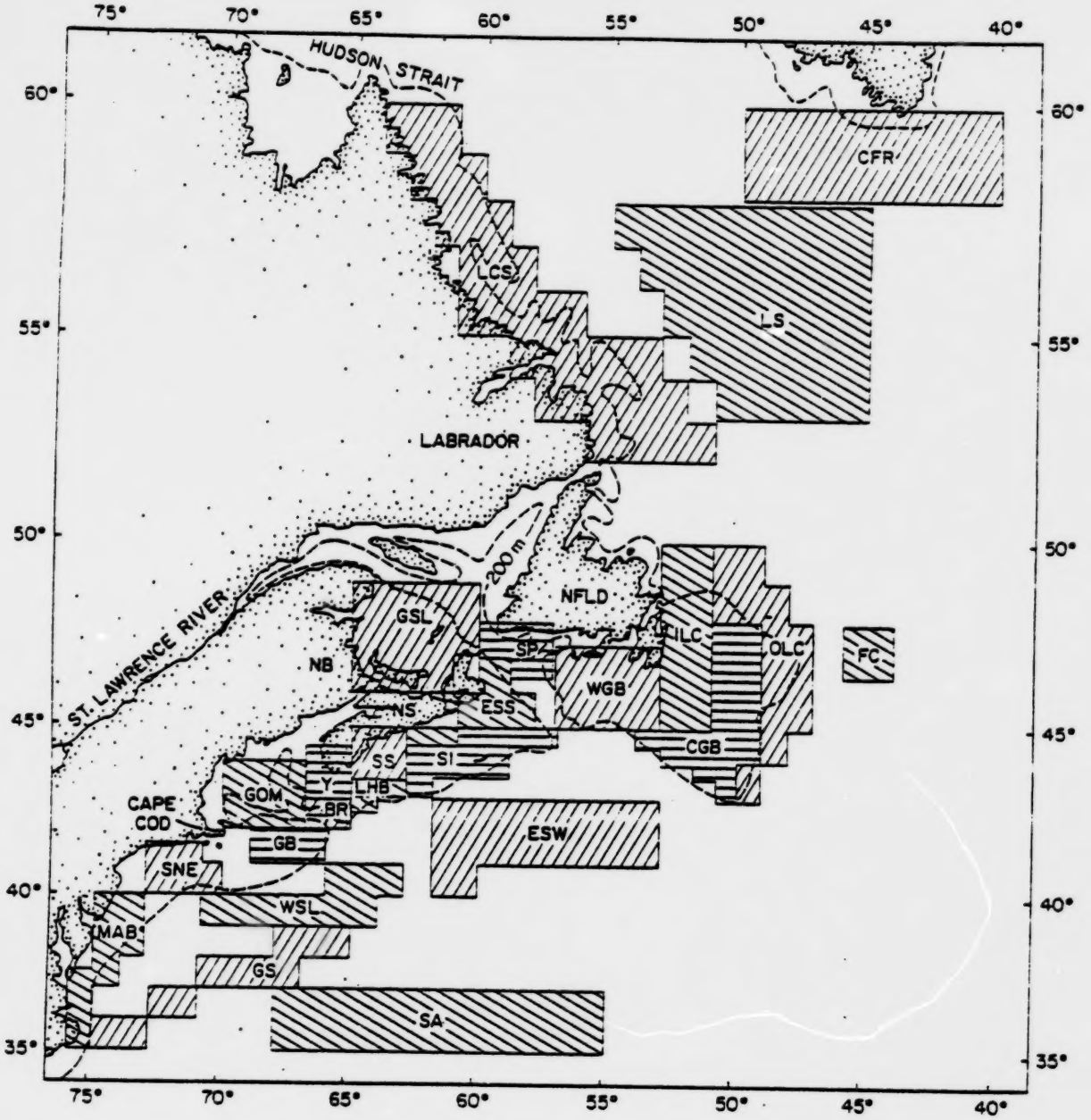

Figure 1 Map of the Northwest Atlantic showing the 24 areas over which SST observations have been averaged monthly.

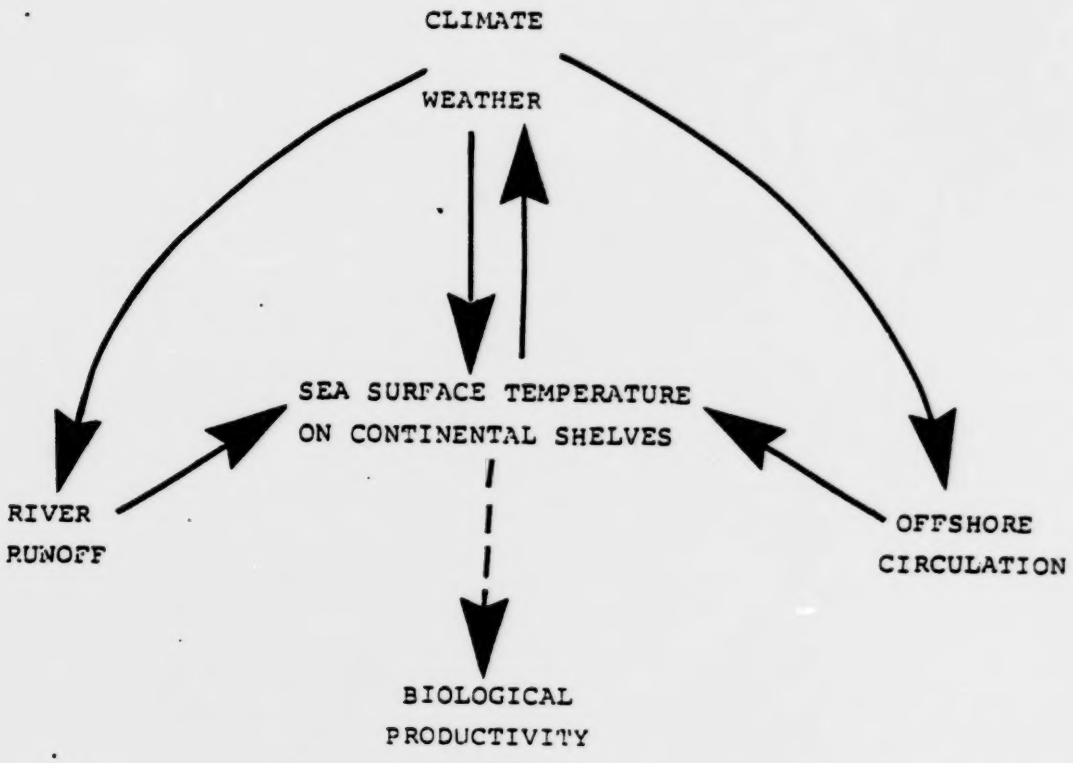

Figure 2 A schematic illustrating the hypothesis that SST's are influenced directly and indirectly by meteorological forcing - the indirect pathways involving either river runoff and coastal waters' stability or the broad ocean gyres and the meanders and rings of the Gulf Stream.

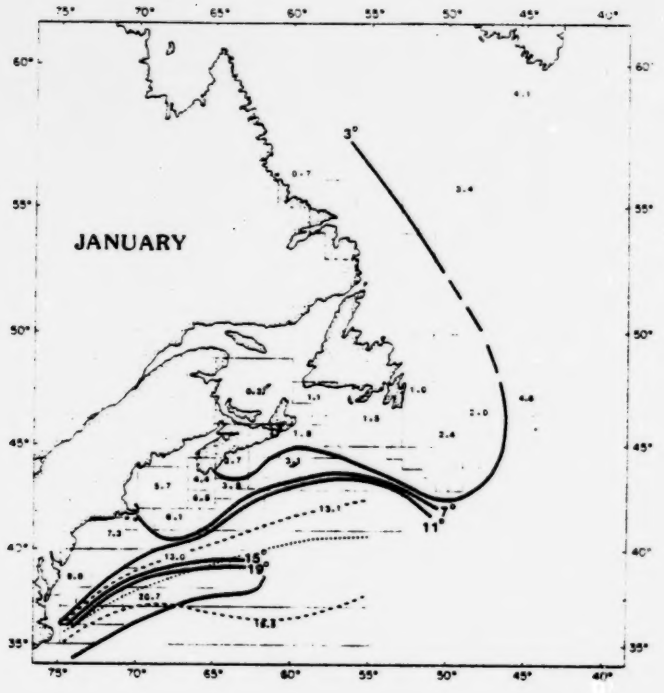

Figure 3(a) Average January Sea Surface Temperature for base period 1946-1980. The long-term mean position (.....) and range limits (----) of the Gulf Stream (Robinson, 1971) are superimposed.

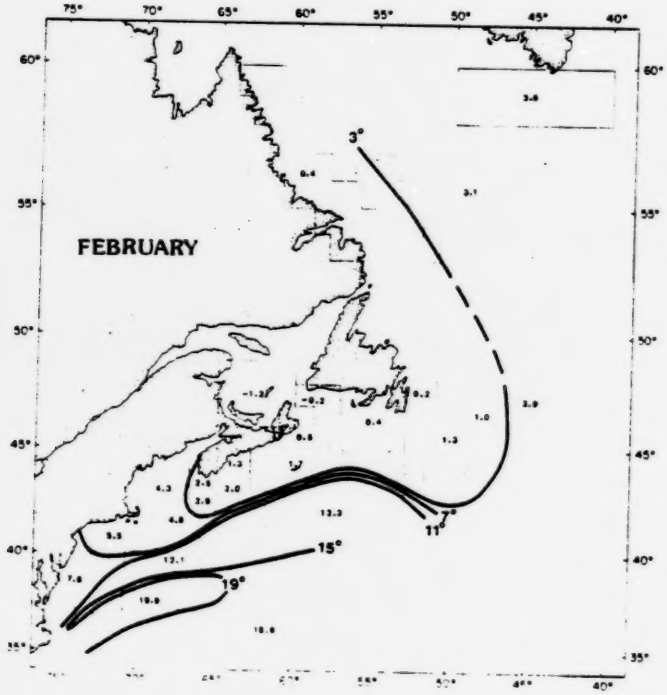

Figure 3(b) Average February Sea Surface Temperature for base period 1946-1980.

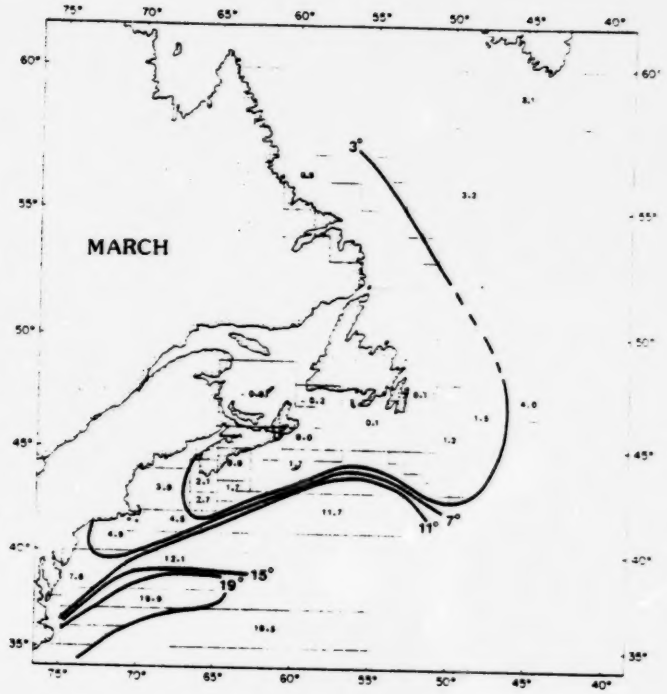

Figure 3(c) Average March Sea Surface Temperature for base period 1946-1980.

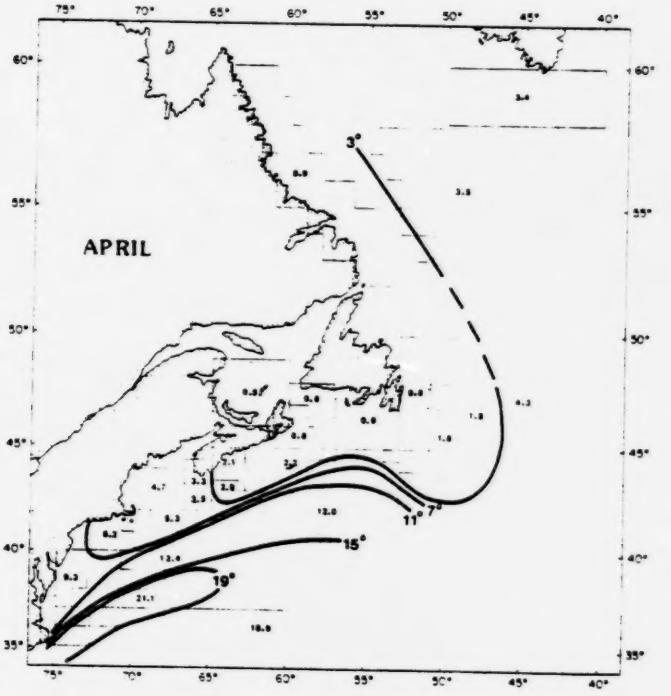

Figure 3(d) Average April Sea Surface Temperature for base period 1946-1980.

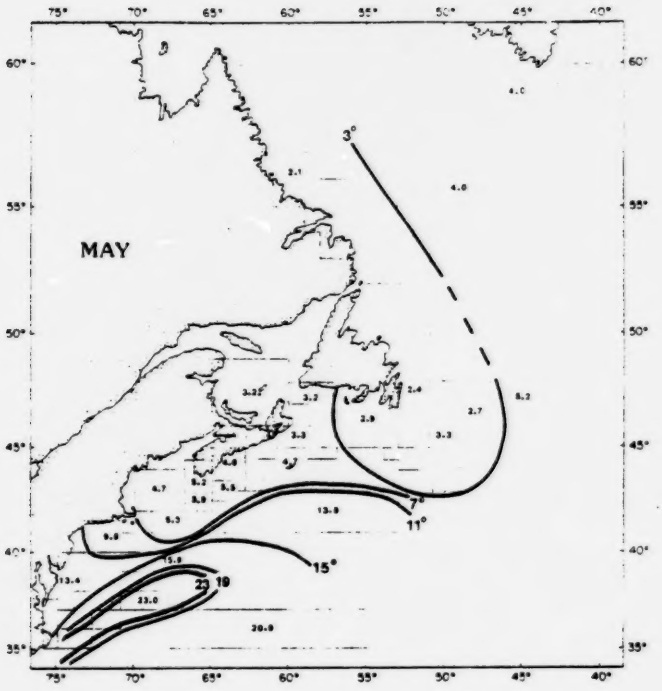

Figure 3(e) Average May Sea Surface Temperature for base period 1946-1980.

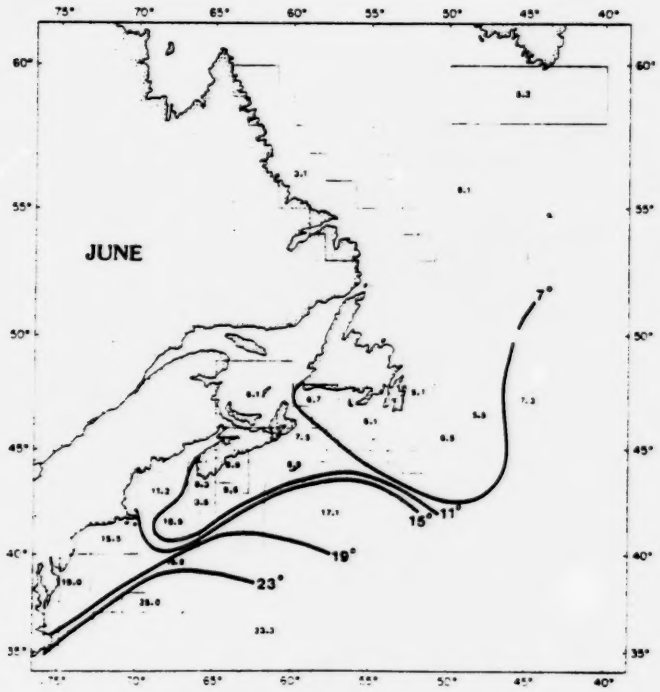

Figure 3(f) Average June Sea Surface Temperature for base period 1946-1980.

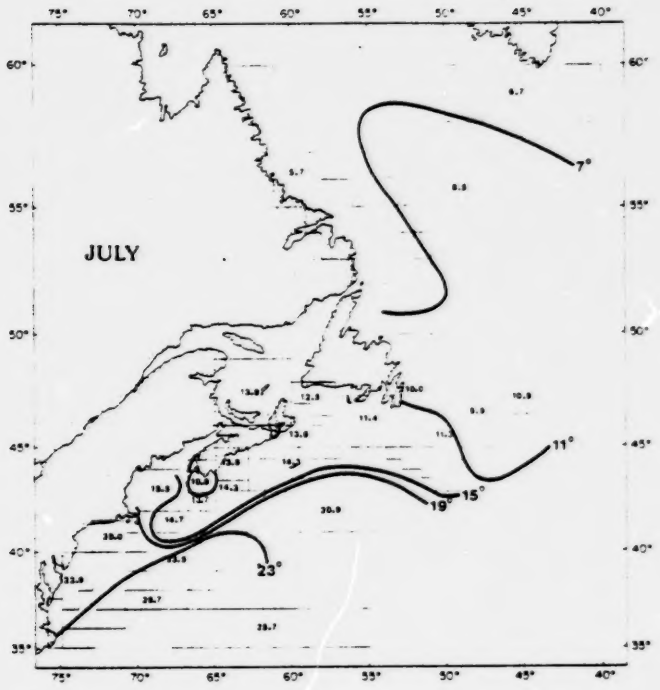

Figure 3(g) Average July Sea Surface Temperature for base period 1946-1980.

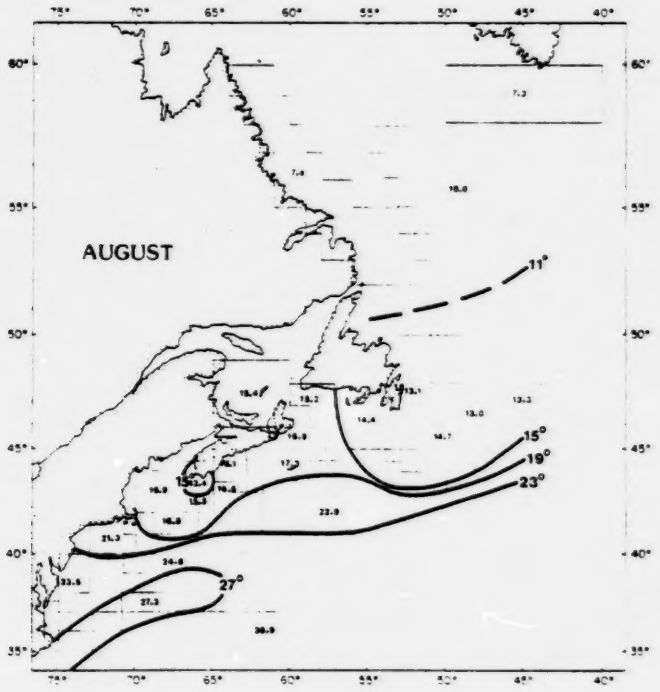

Figure 3(h) Average August Sea Surface Temperature for base period 1946-1980.

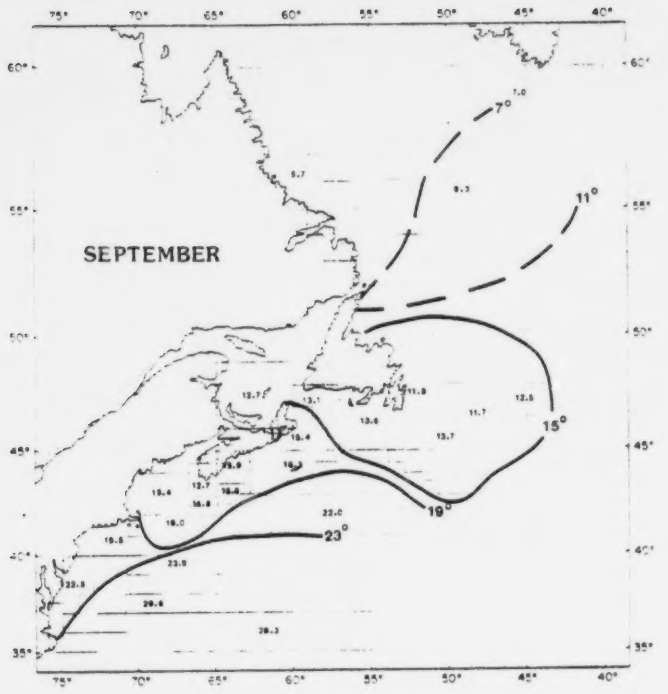

Figure 3(i) Average September Sea Surface Temperature for base period 1946-1980.

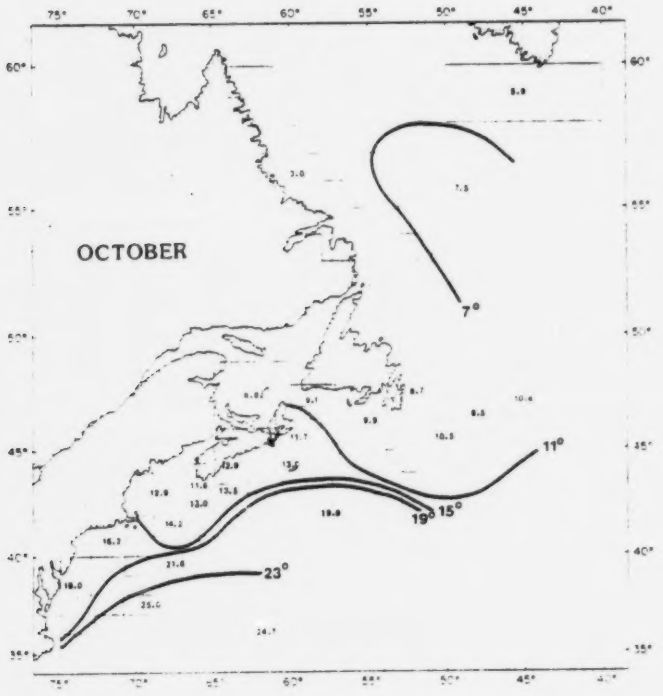

Figure 3(j) Average October Sea Surface Temperature for base period 1946-1980.

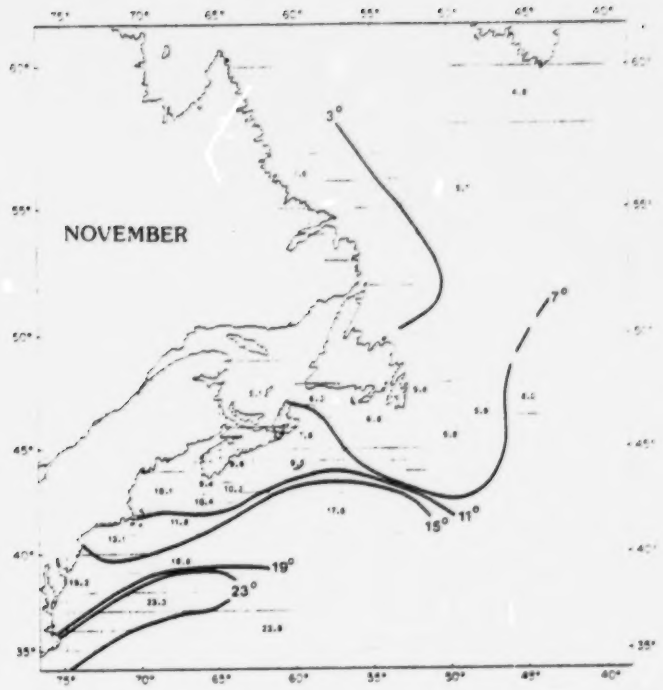

Figure 3(k) Average November Sea Surface Temperature for base period 1946-1980.

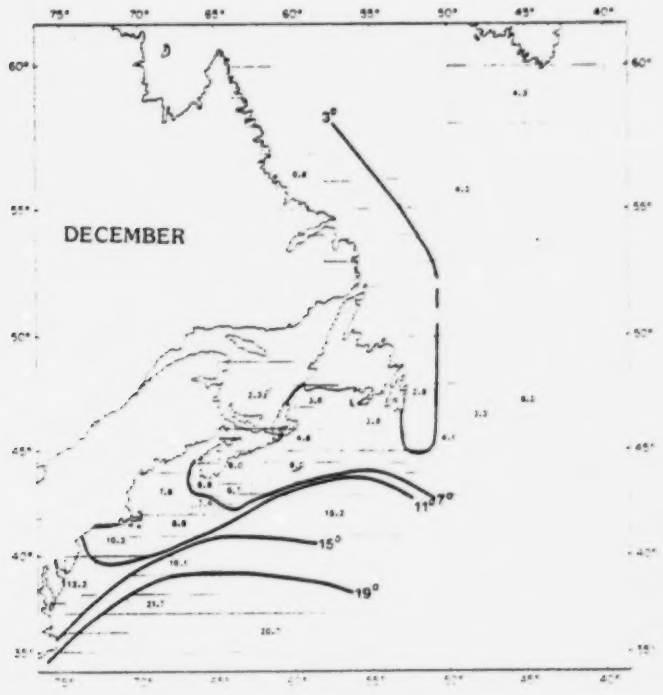

Figure 3(l) Average December Sea Surface Temperature for base period 1946-1980.

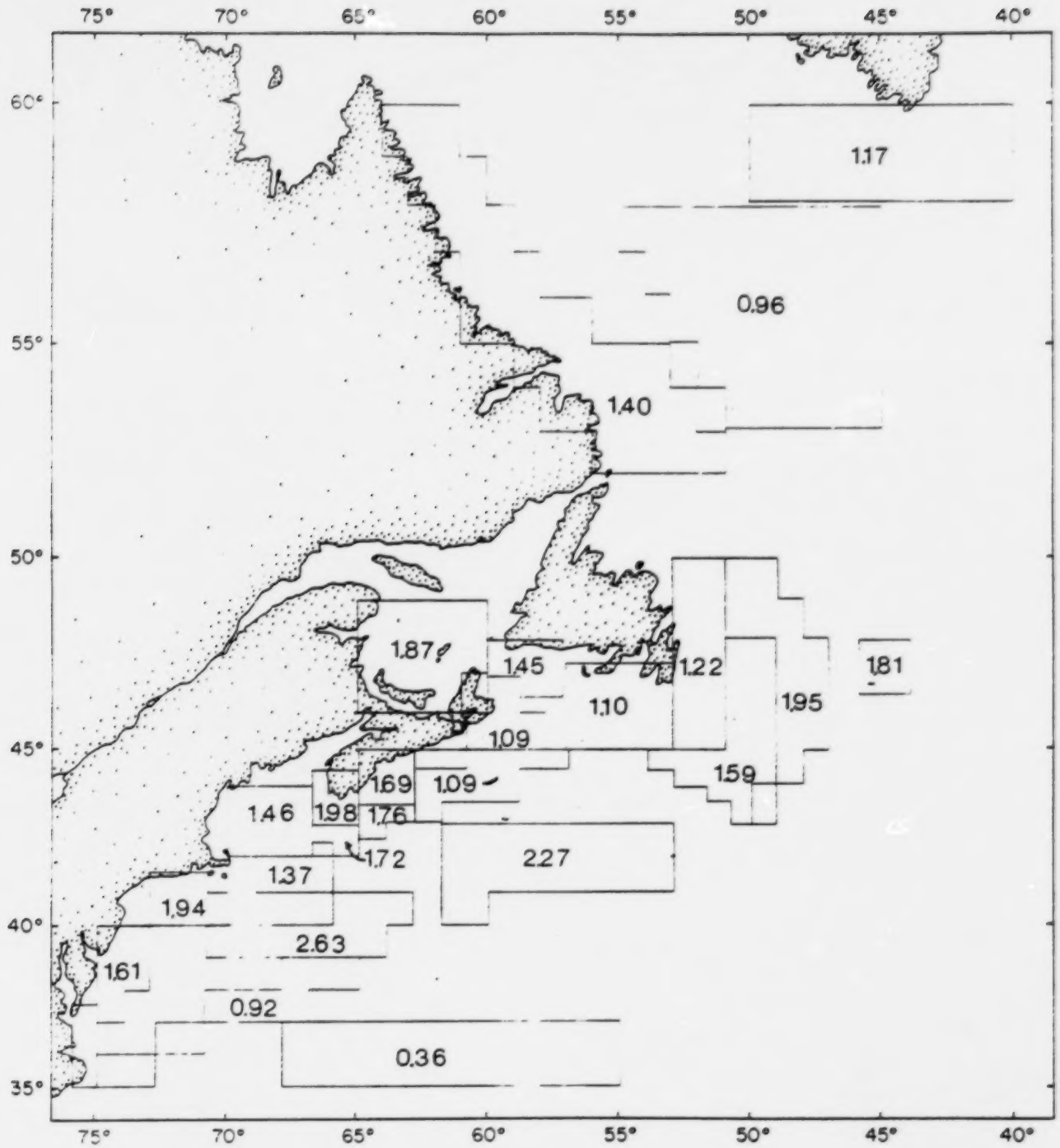

Figure 4 Variance of the SST signal (deseasonalized version) by area in Celsius degrees squared.

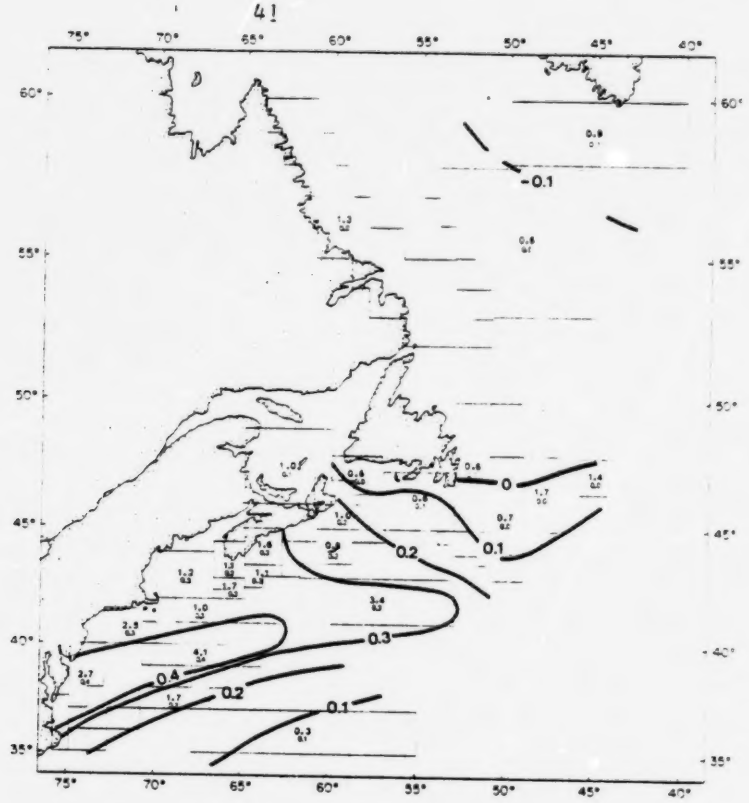

Figure 5 Map of the seasonal (N x 3) variance (upper numbers, degrees squared) and the first mode eigenvector coefficients (lower numbers and contours) for winter (January, February, March).

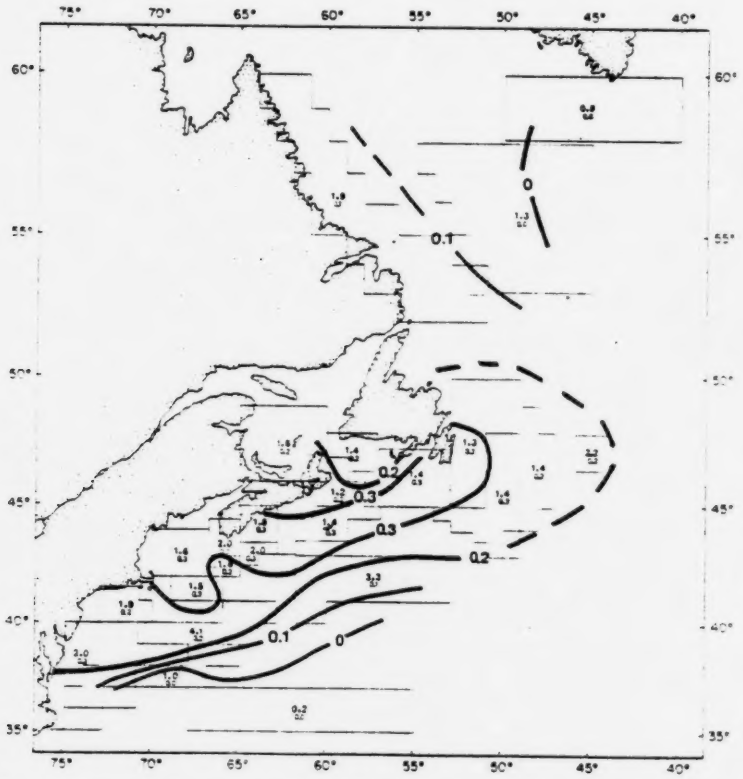

Figure 6 Map of the seasonal (N x 3) variance (upper numbers, degrees squared) and the first mode eigenvector coefficients (lower numbers and contours) for spring (April, May, June).

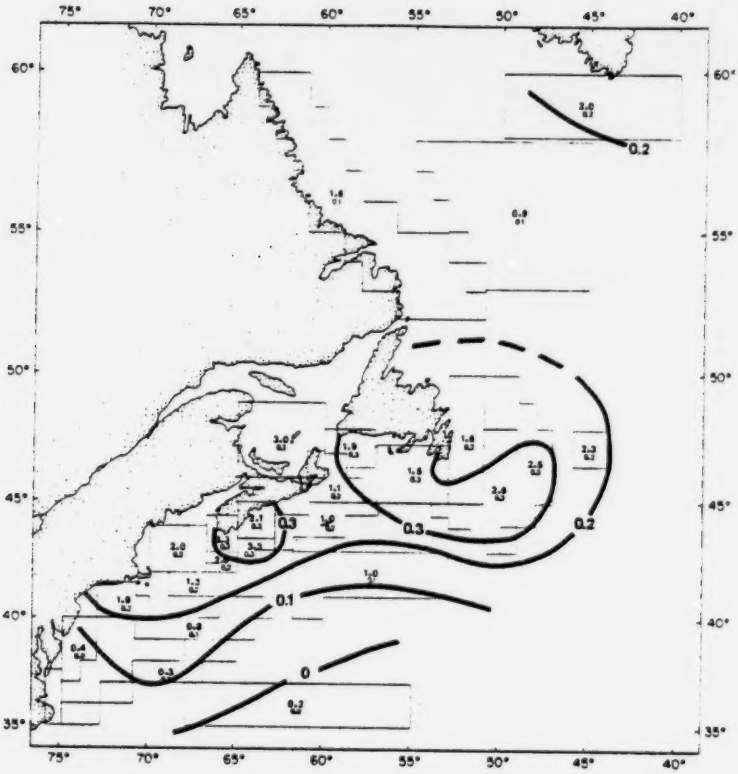

Figure 7 Map of the seasonal (N x 3) variance (upper numbers, degrees squared) and the first mode eigenvector coefficients (lower numbers and contours) for summer (July, August, September).

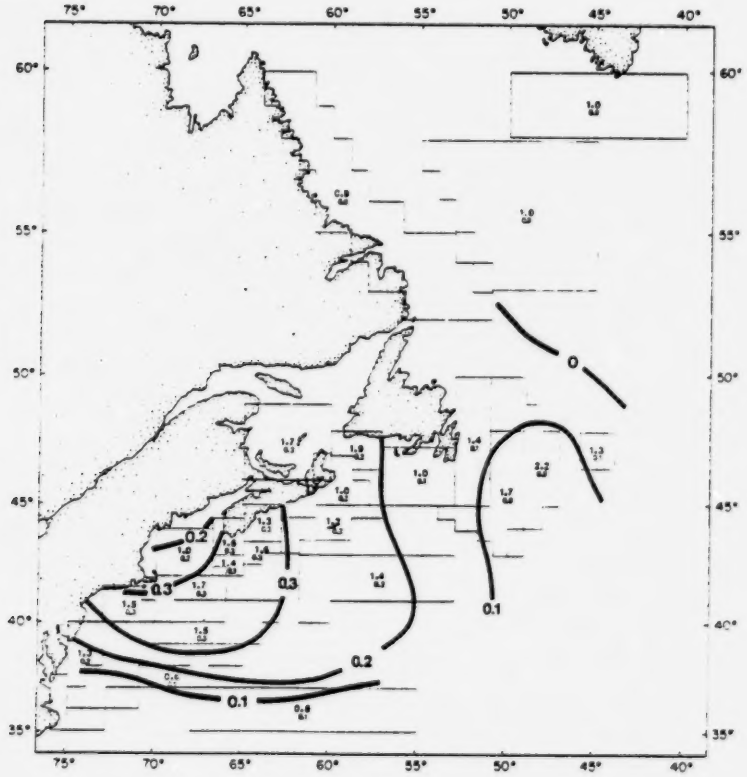

Figure 8 Map of the seasonal (N x 3) variance (upper numbers, degrees squared) and the first mode eigenvector coefficients (lower numbers and contours) for autumn (October, November, December).

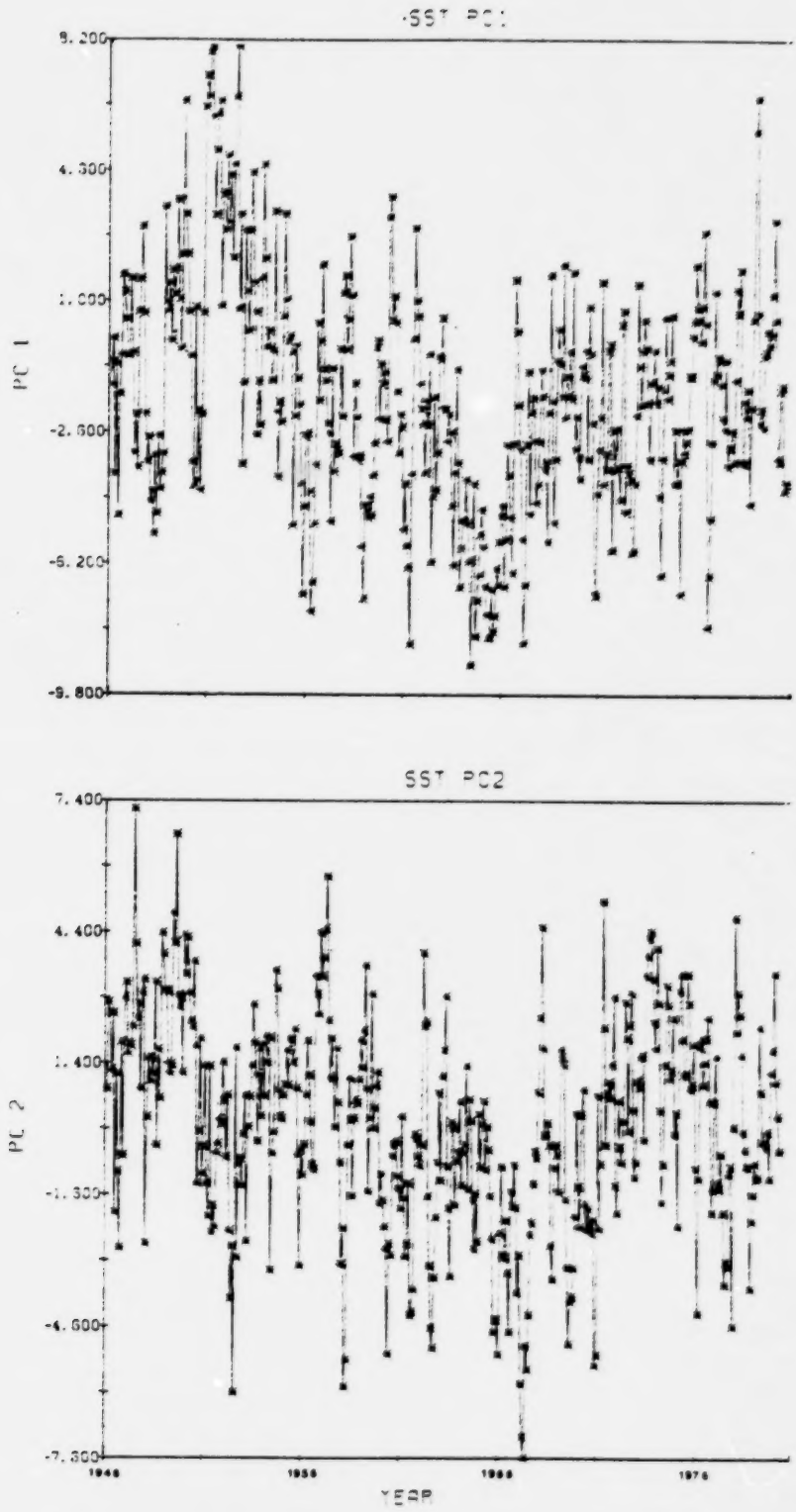

Figure 9 Time series plots of monthly time series of first (PC1) and second (PC2) EOF (N x 12) modes for period 1946-1980).

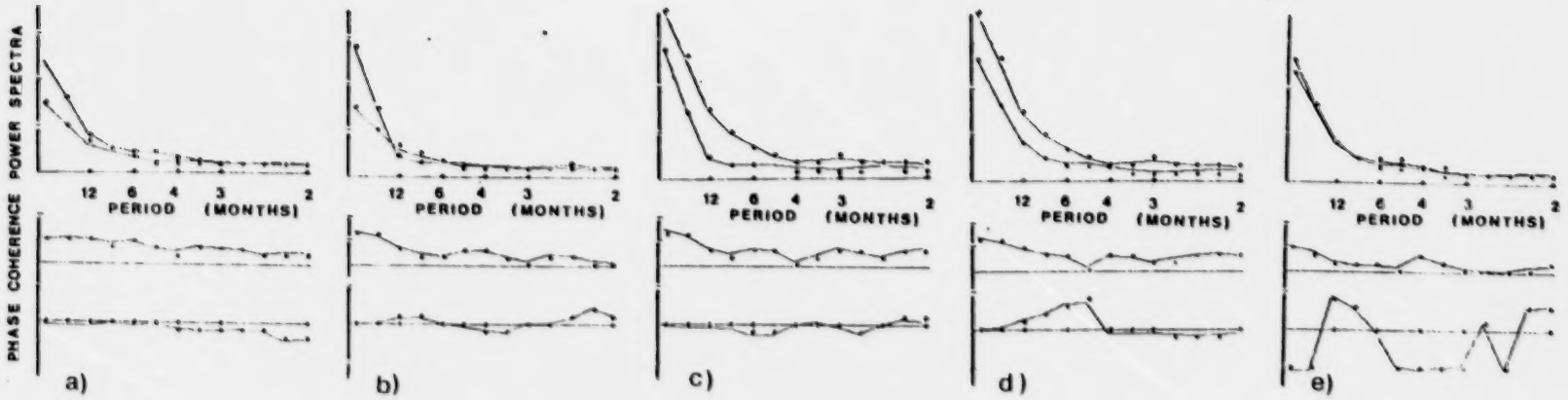

Figure 10 Power spectra, coherence and phase for paris of SST (N x 12) signals. (a) Central Grand Bank (.) and Eastern Shore (+). (b) Eastern Shore (+) and Georges Bank (.). (c) Georges Bank (.) and Western Slope (+). (d) Western Slope (+) and mid-Atlantic Bight (.). (e) Mid-Atlantic Bight (+) and Central Grand Bank (.). The 95% significance threshold for coherence, 0.26, is drawn in for comparison.

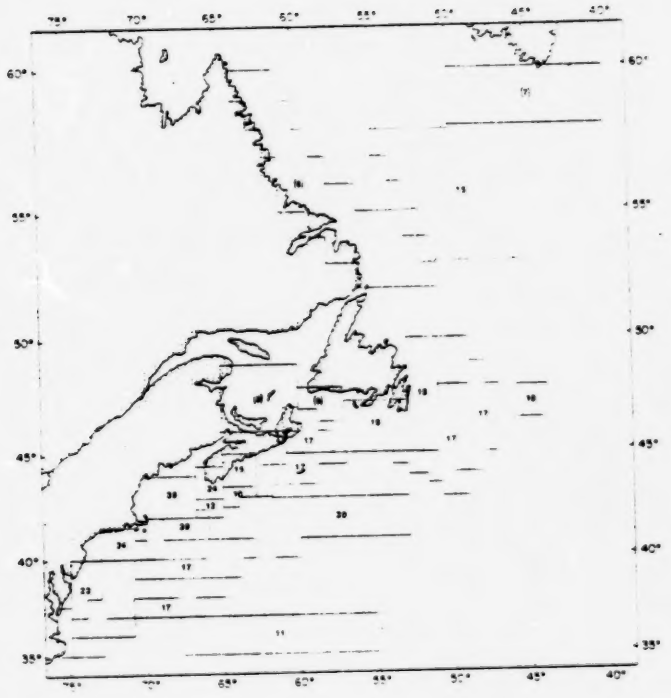

Figure 11 Graphs showing the half-power period of SST months, calculated from the power spectra.

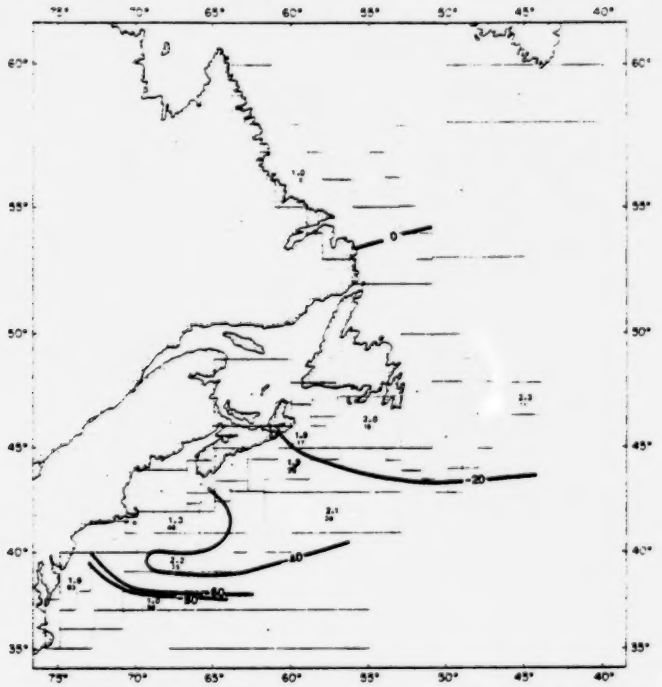

Figure 12 Map showing the amplitude (upper numbers) and phase (degrees of lag; lower numbers and contours) for the first mode, CEOF (N x 12), 12 month band.

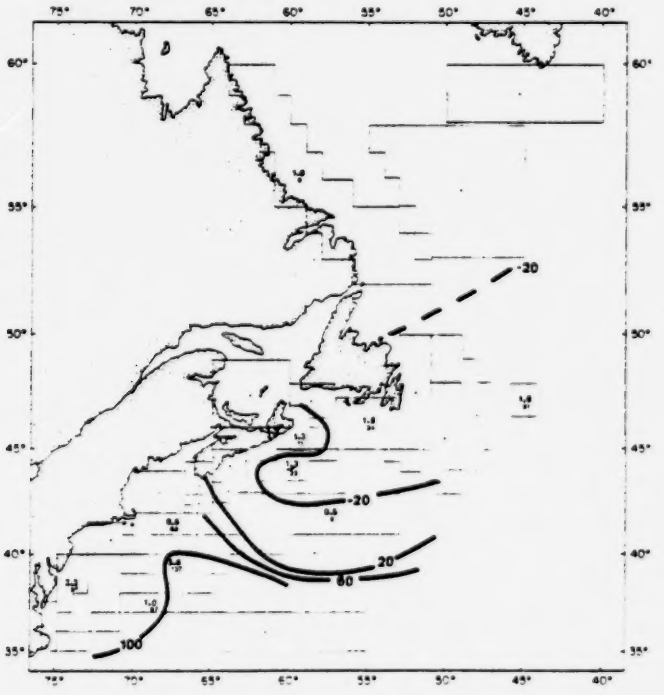

Figure 13 Map showing the amplitude (upper numbers) and phase (degrees of lag; lower numbers and contours) for the second mode, CEOF (N x 12), 12 month band.

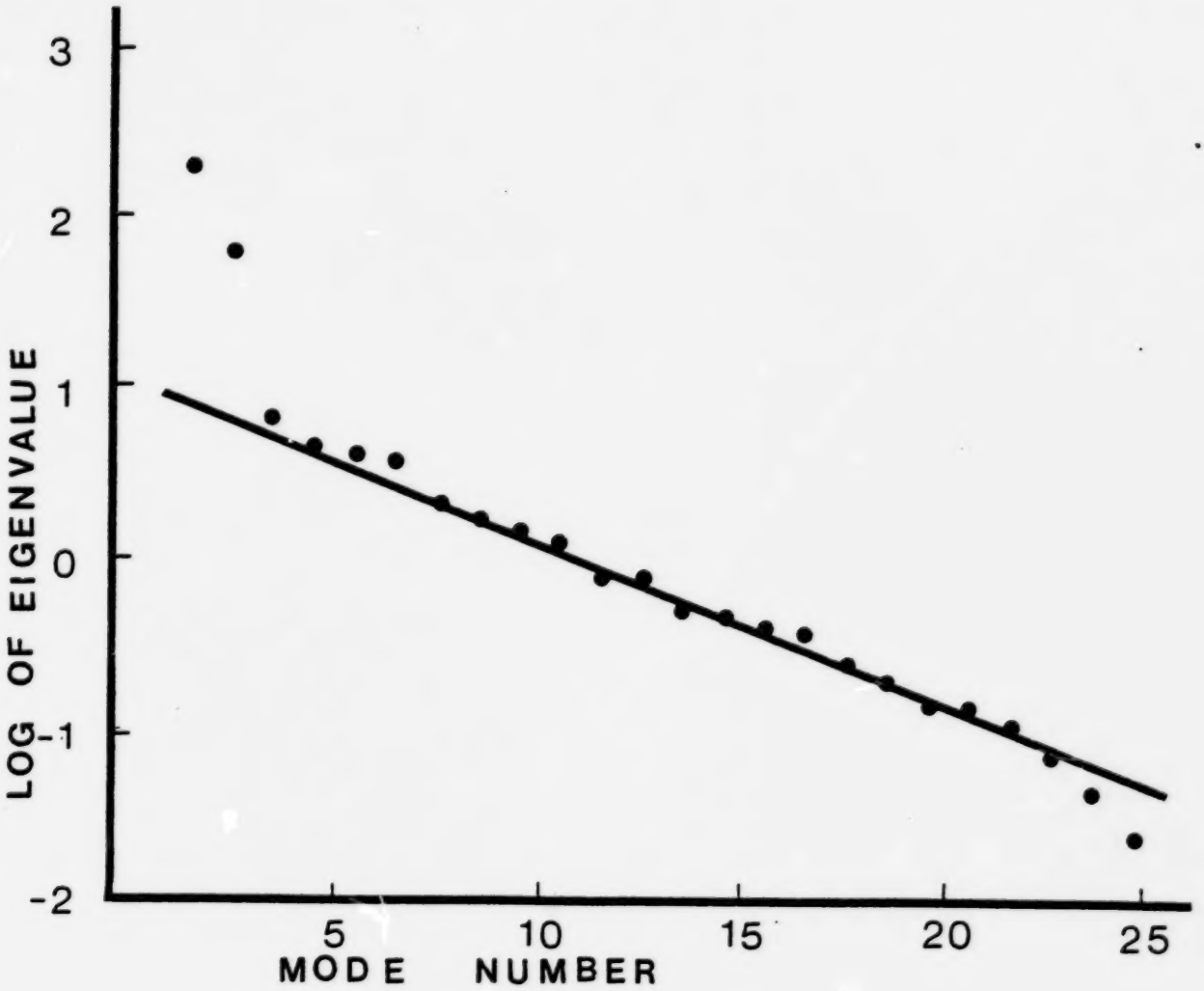

Figure 14 Semi-logarithmic plot of (N x 12) eigenvalues versus mode number.

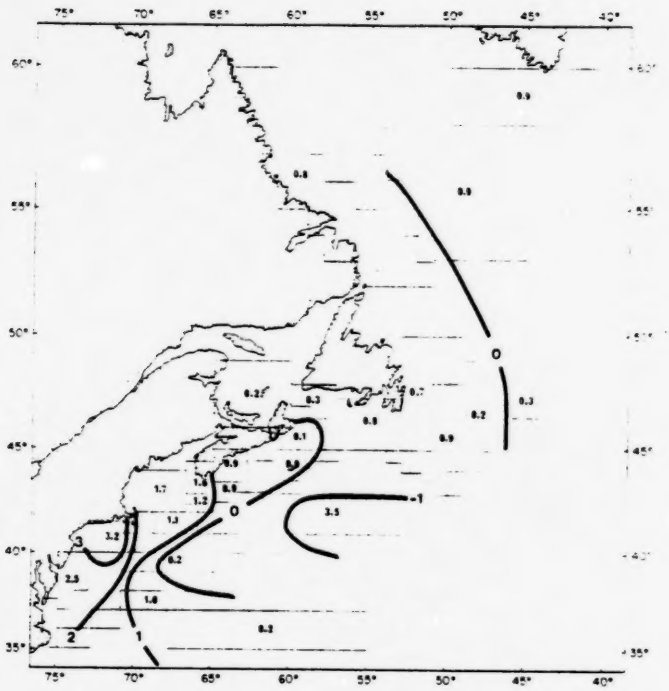

Figure 15(a) Map of GSST anomalies (°C) for February, 1950.

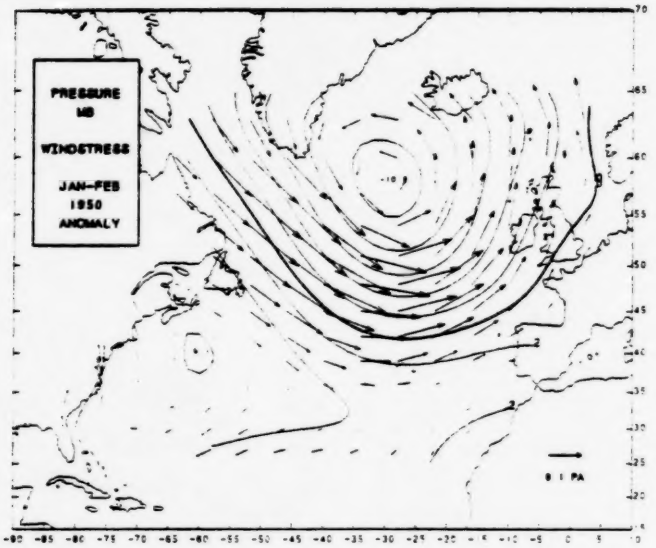

Figure 15(b) Map of atmospheric pressure and wind stress anomalies for January-February, 1950 (from Thompson and Hazen, 1983).

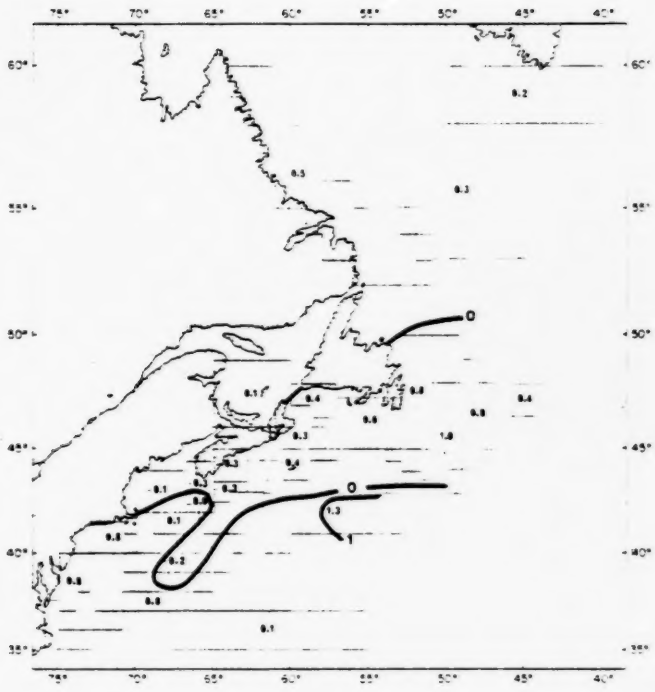

Figure 16 Map of GSST anomalies (°C) for August, 1950.

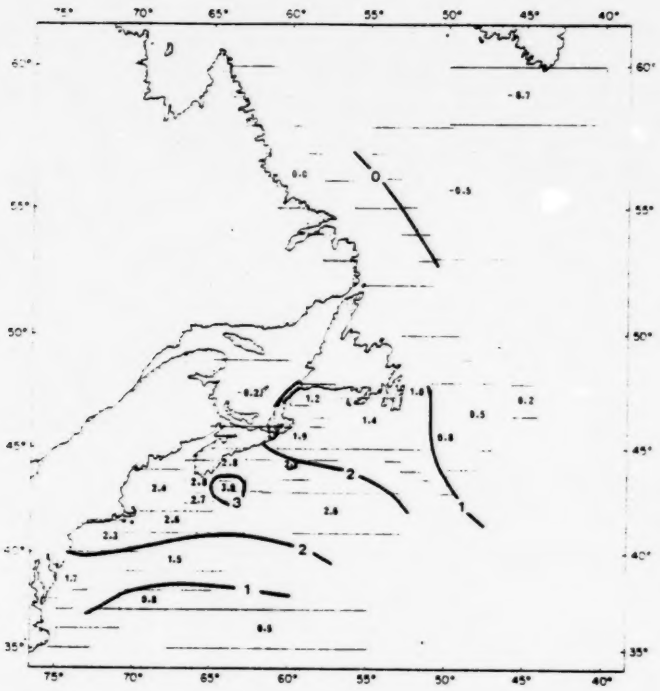

Figure 17(a) Map of GSST anomalies (°C) for February, 1951.

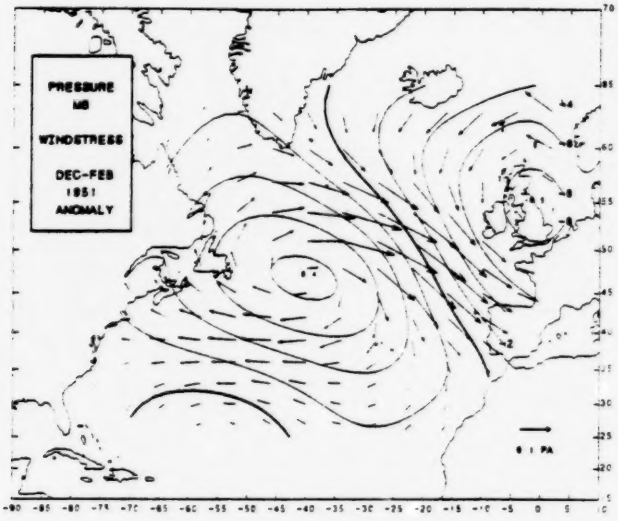

Figure 17(b) Map of atmospheric pressure and wind stress anomalies for December, 1950 -February 1951 period.

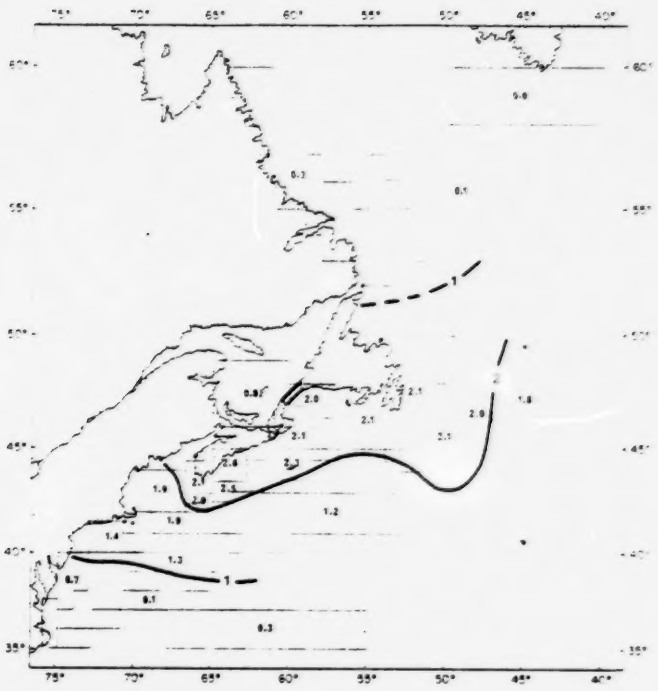

Figure 18(a) Map of GSST anomalies (°C) for August, 1951.

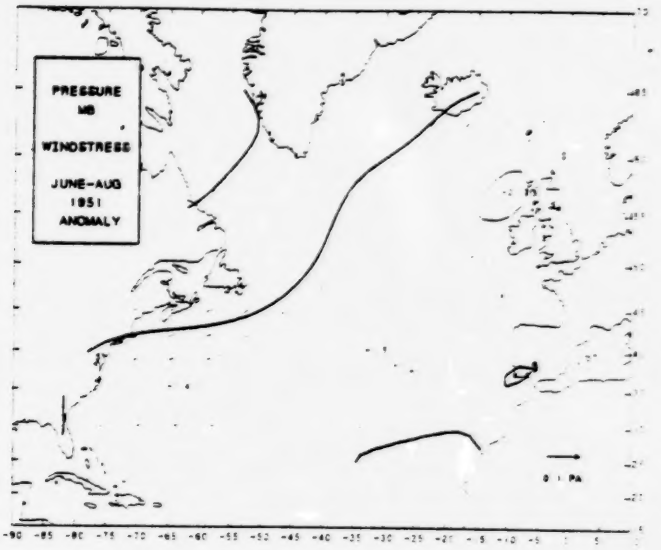

Figure 18(b) Map of atmospheric pressure and wind stress anomalies for June-August, 1951 period.

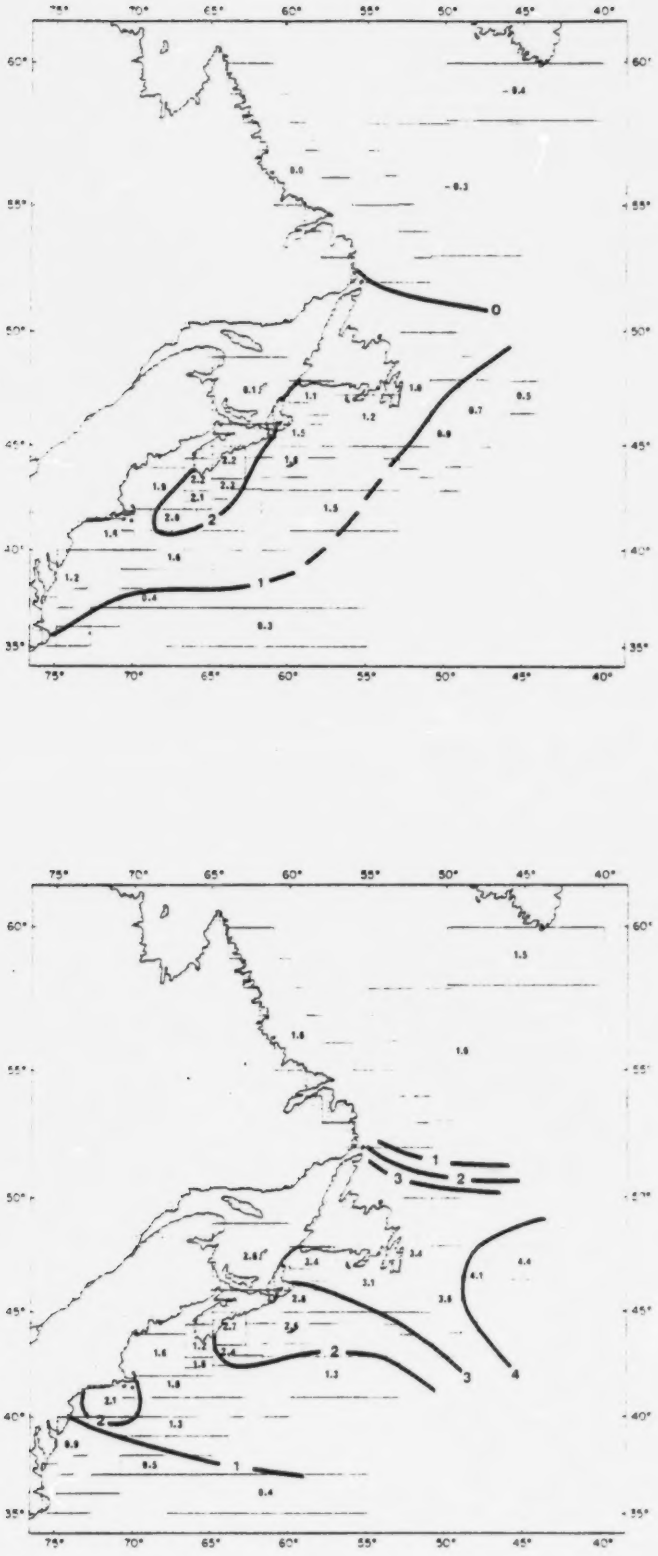

Figure 19 Map of GSST anomalies (°C) for February, 1952 (upper) and August, 1952 (lower).

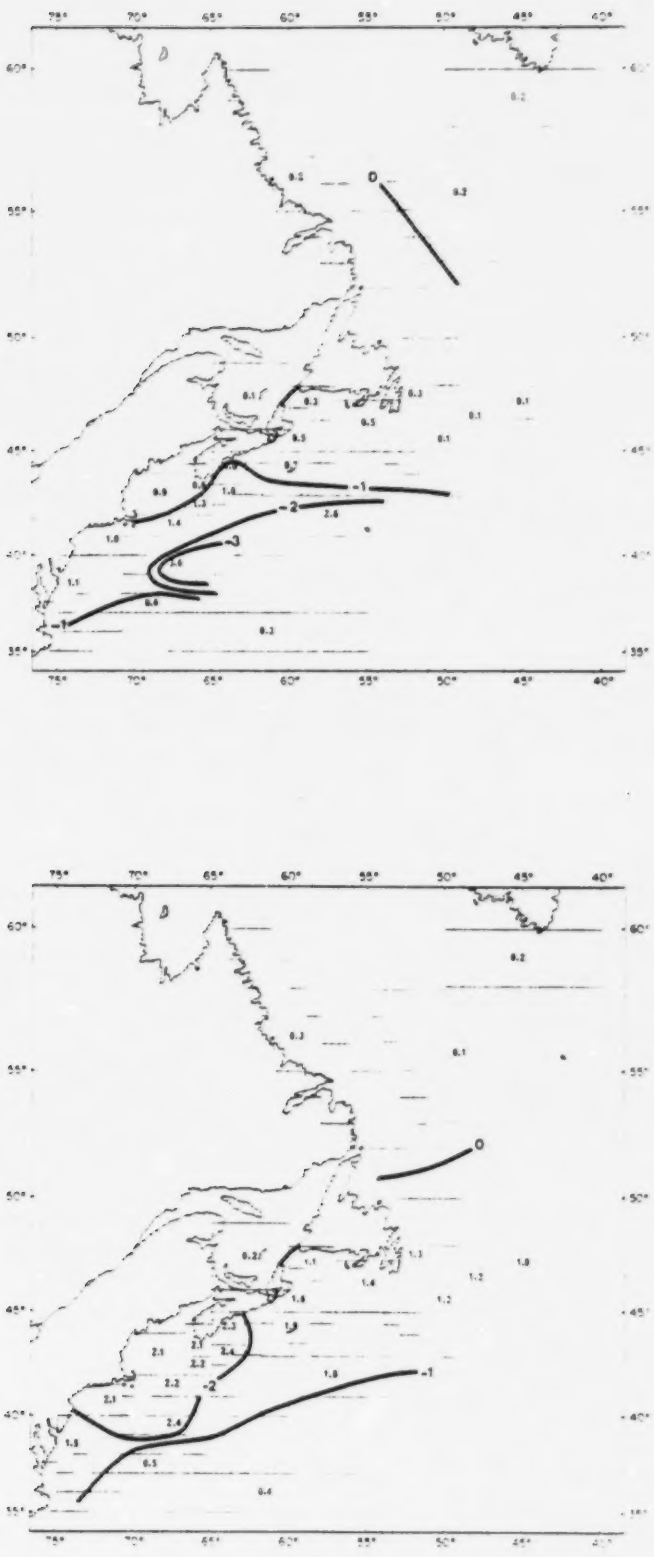

Figure 20 Map of GSST anomalies (°C) for February, 1964 (upper) and August, 1964 (lower).

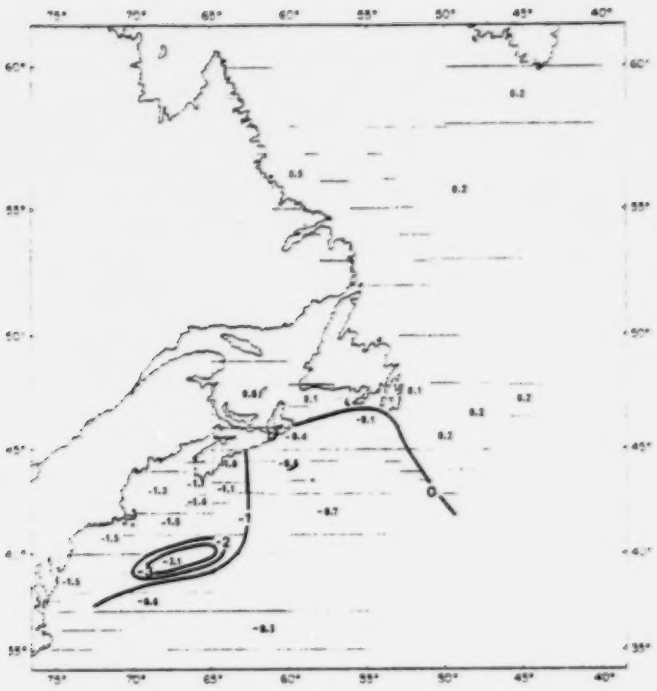

Figure 21(a) Map of GSST anomalies (°C) for February, 1965.

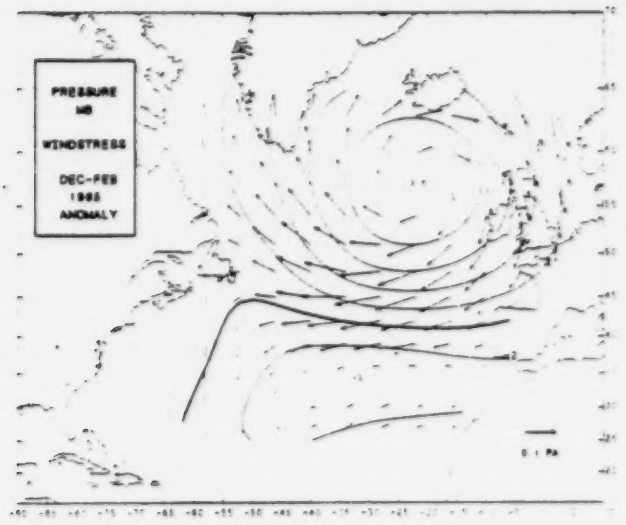

Figure 21(b) Map of atmospheric pressure and wind stress anomalies for December, 1964 -February, 1965 period.

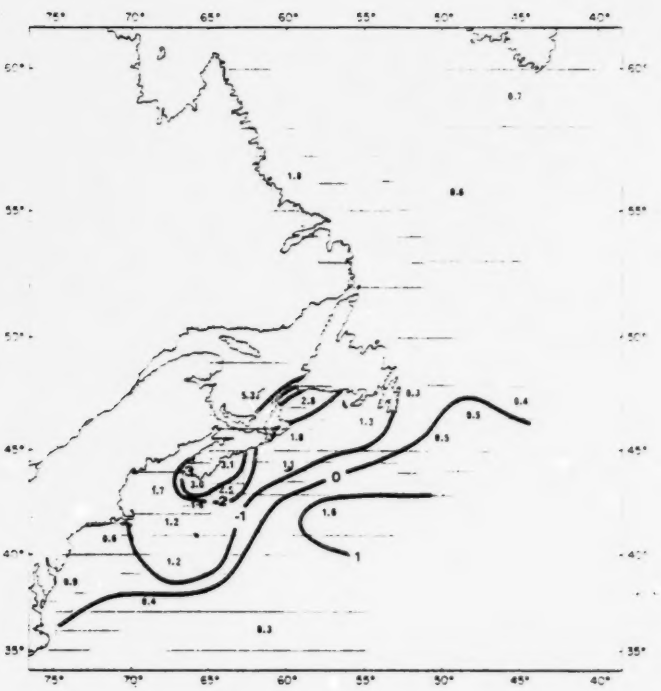

Figure 22(a) Map of GSST anomalies (°C) for August, 1965.

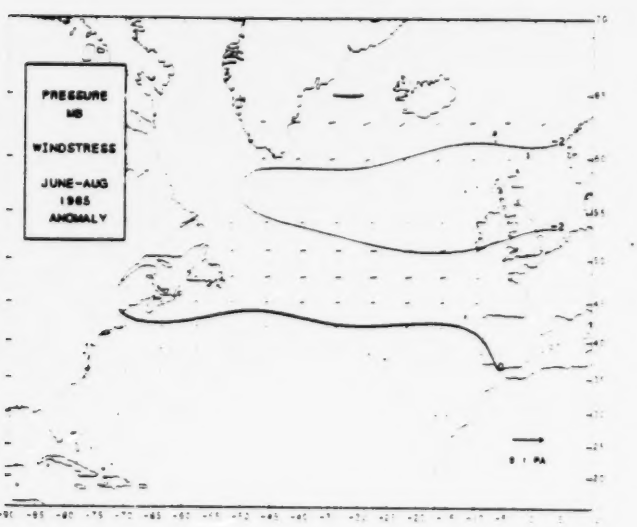

Figure 22(b) Map of atmospheric pressure and wind stress anomalies for June-September, 1965 period.

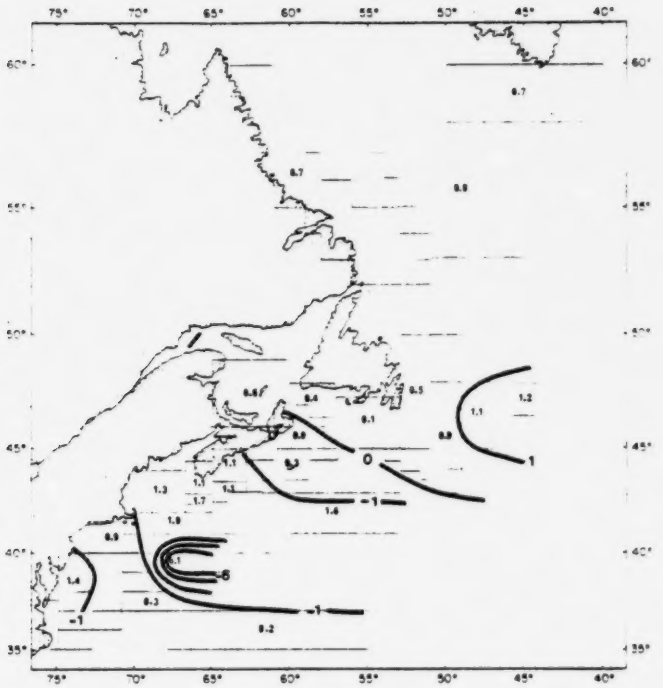

Figure 23(a) Map of GSST anomalies (°C) for February, 1966.

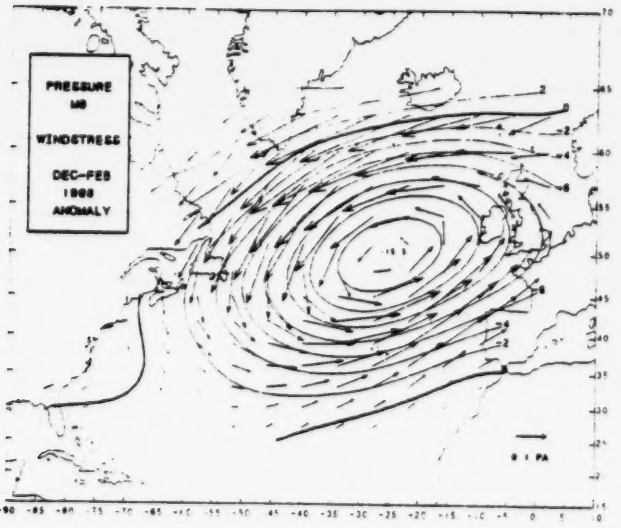

Figure 23(b) Map of atmospheric pressure and wind stress anomalies for December, 1965 -February, 1966 period.

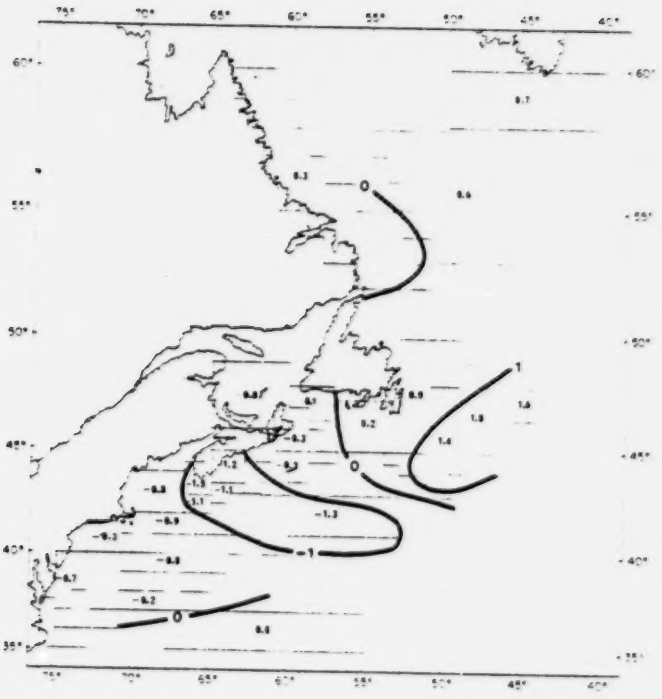

Figure 24 Map of GSST anomalies (°C) for August, 1966.

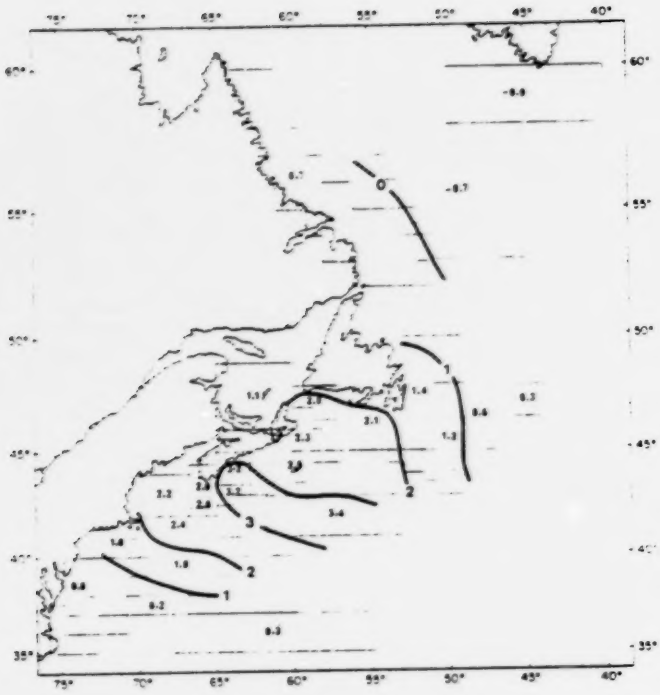

Figure 25(a) Map of GSST anomalies (°C) for January, 1951.

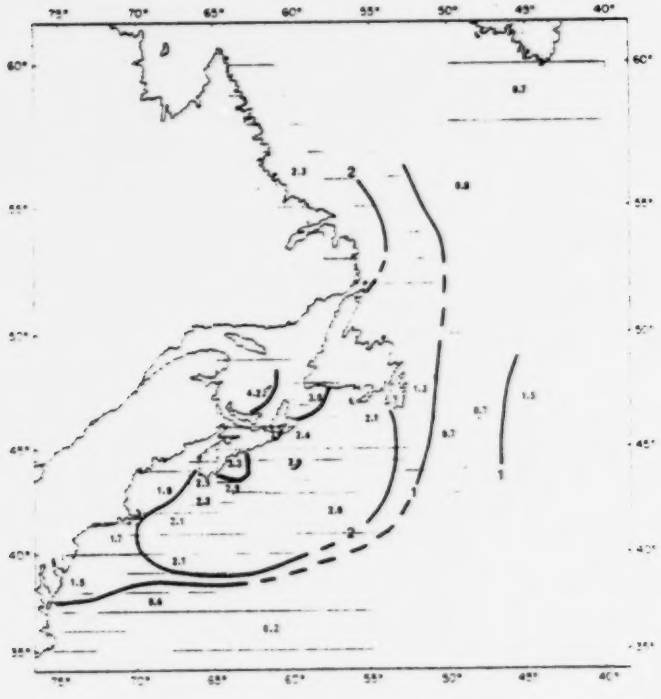

Figure 25(b) Map of GSST anomalies (°C) for February, 1951.

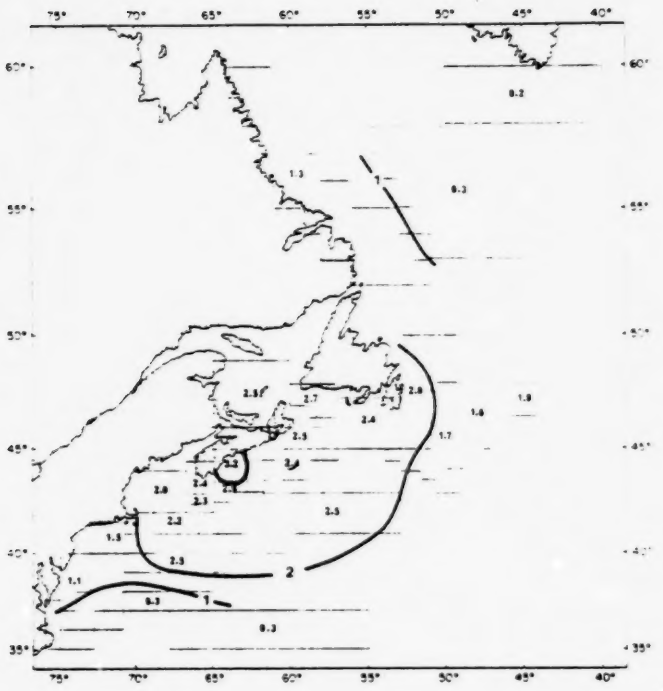

Figure 25(c) Map of GSST anomalies (°C) for March, 1951.

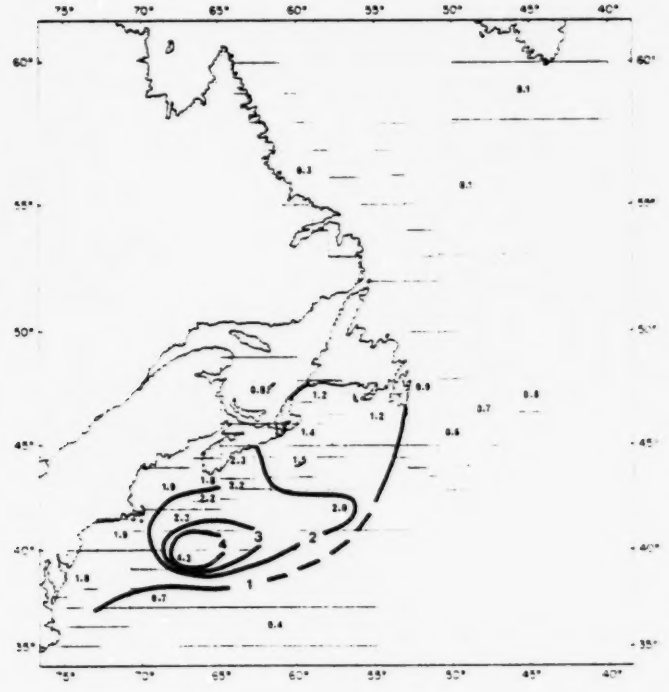

Figure 25(d) Map of GSST anomalies (°C) for April, 1951.

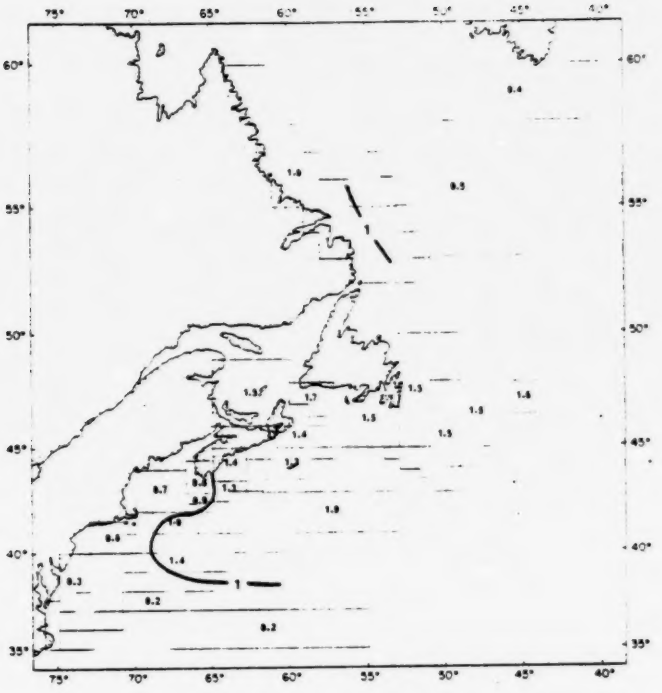

Figure 25(e) Map of GSST anomalies (°C) for May, 1951.

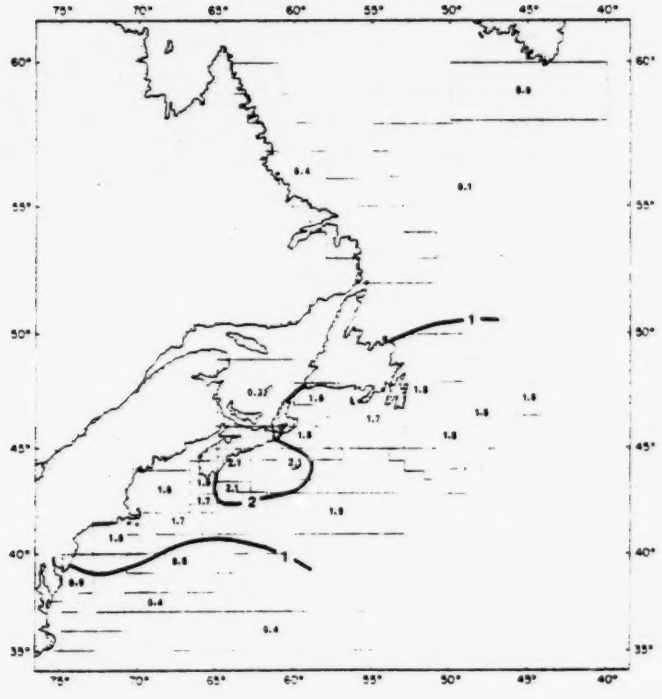

Figure 25(f) Map of GSST anomalies (°C) for June, 1951.

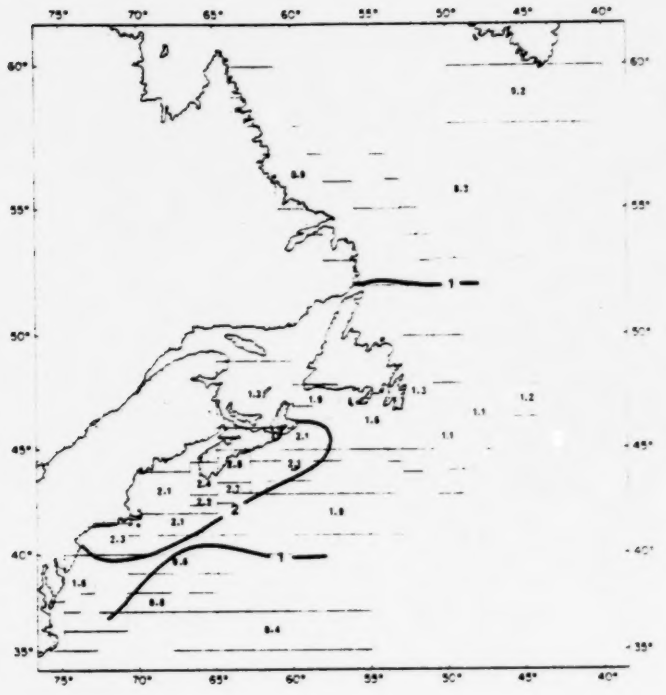

Figure 25(g) Map of GSST anomalies (°C) for July, 1951.

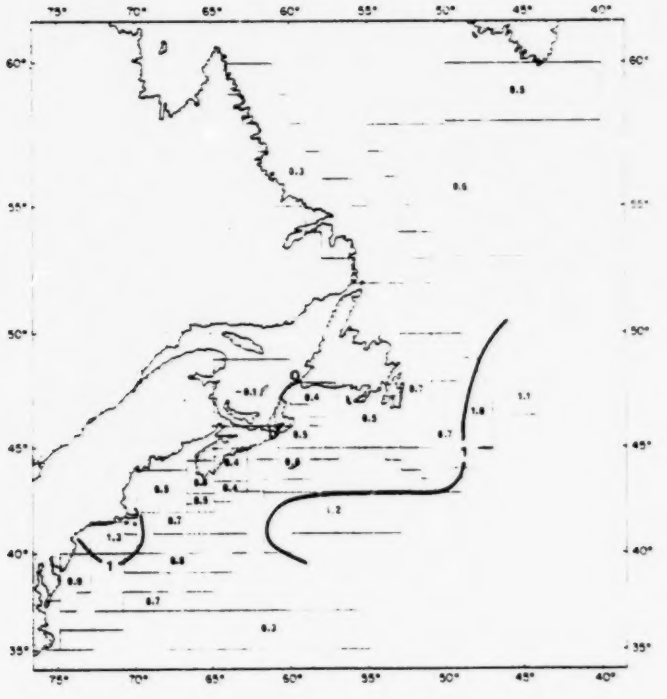

Figure 25(h) Map of GSST anomalies (°C) for August, 1951.

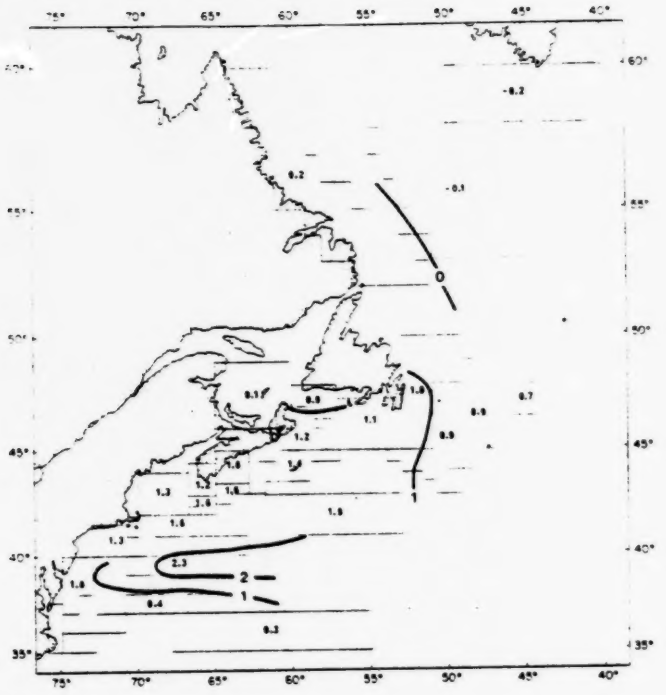

Figure 25(i) Map of GSST anomalies (°C) for September, 1951.

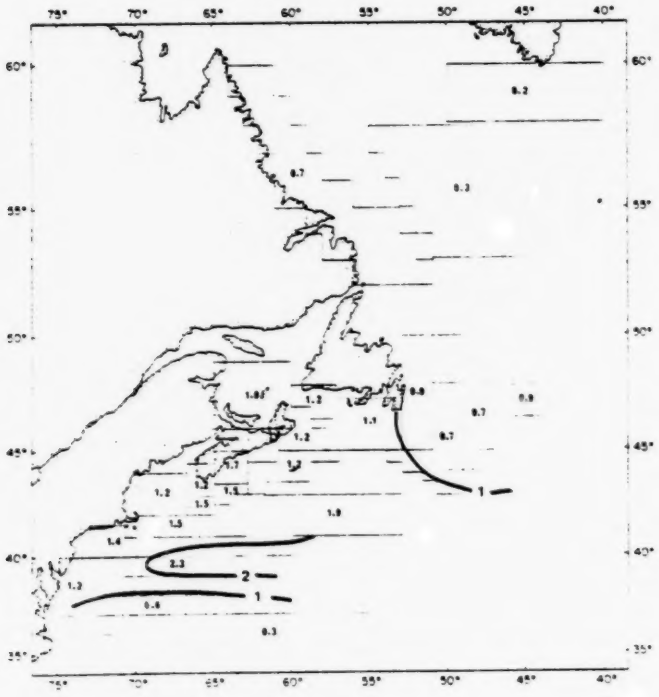

Figure 25(j) Map of GSST anomalies (°C) for October, 1951.

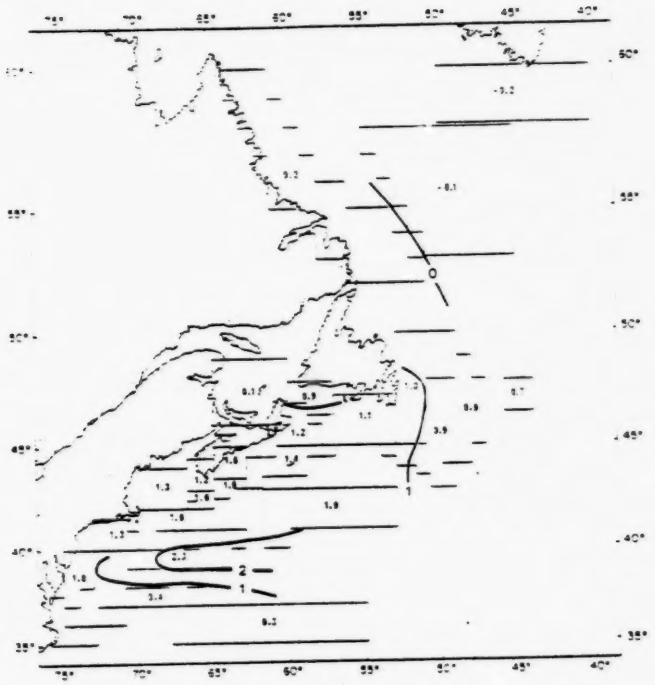

Figure 25(k) Map of GSST anomalies (°C) for November, 1951.

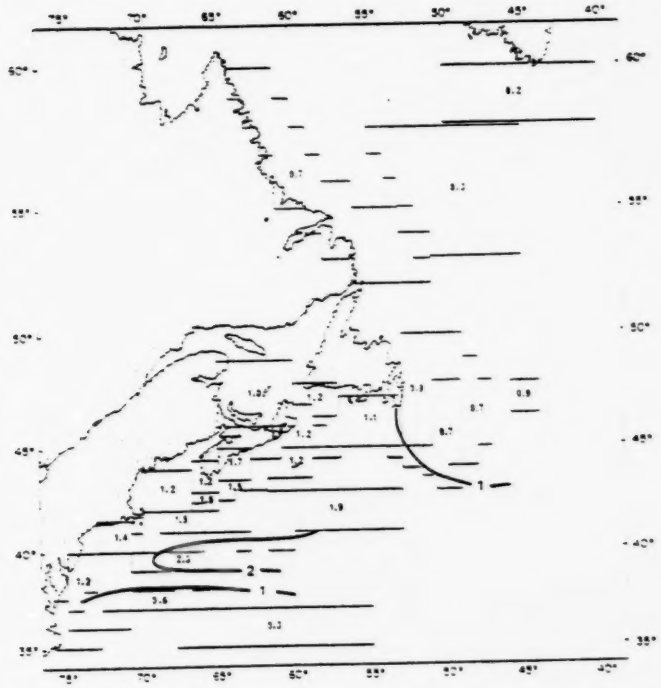

Figure 25(l) Map of GSST anomalies (°C) for December, 1951.

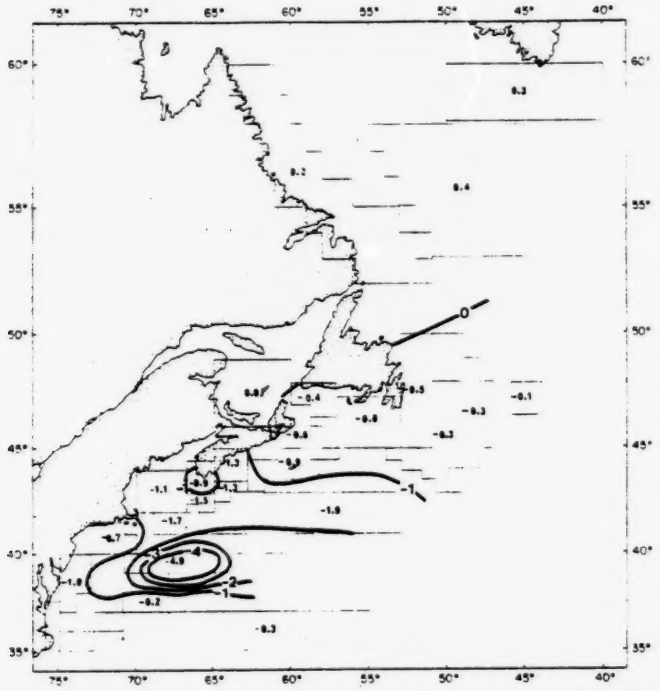

Figure 26(a) Map of GSST anomalies (°C) for January, 1965.

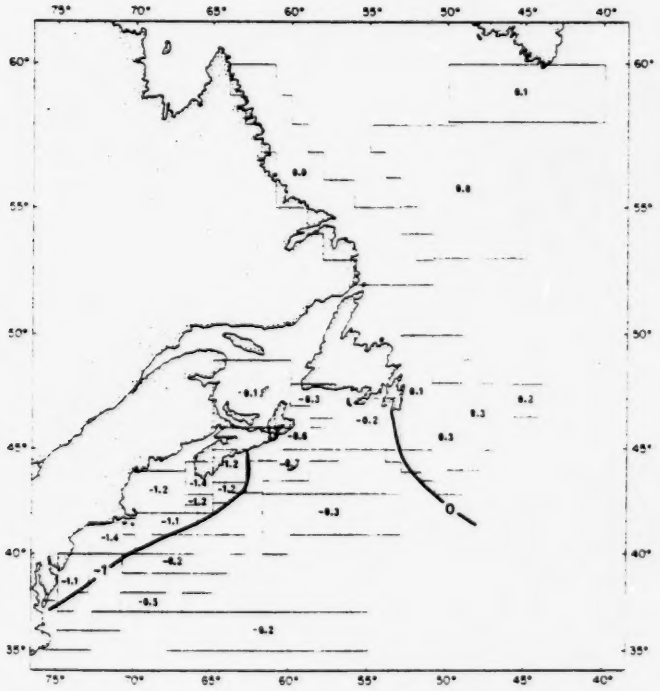

Figure 26(b) Map of GSST anomalies (°C) for February, 1965.

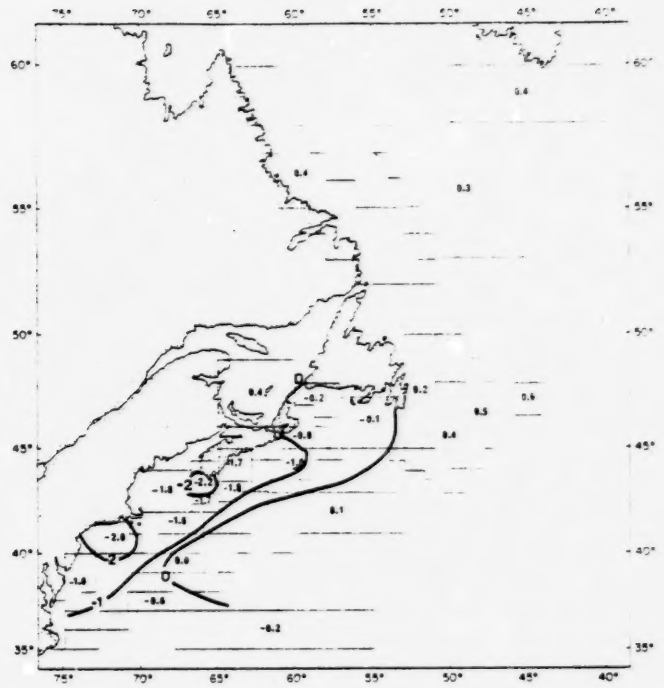

Figure 26(c) Map of GSST anomalies (°C) for March, 1965.

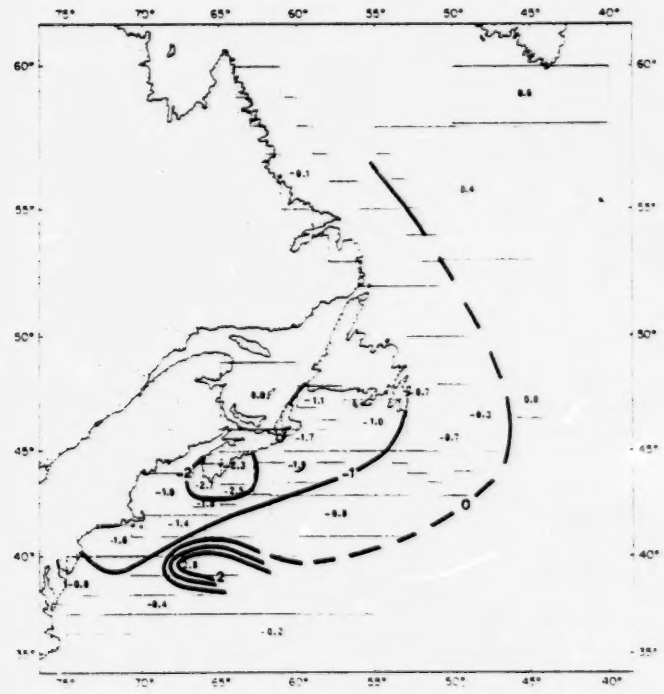

Figure 26(d) Map of GSST anomalies (°C) for April, 1965.

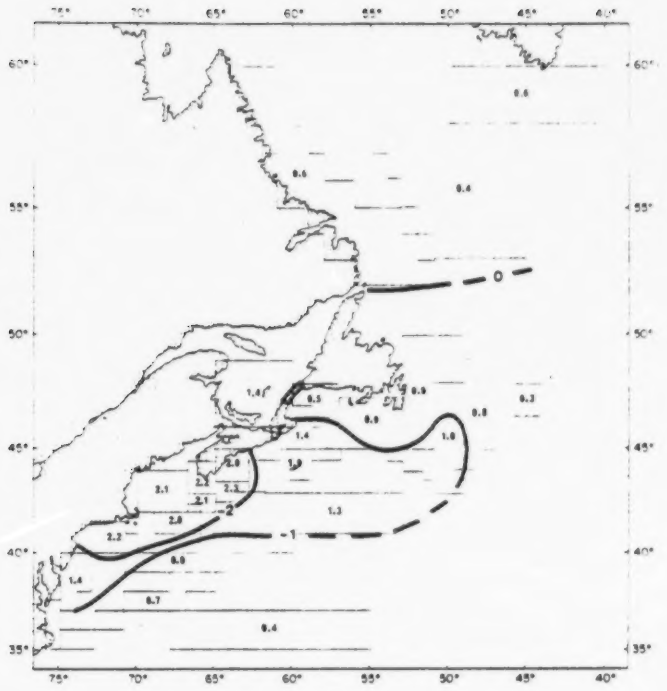

Figure 26(e) Map of GSST anomalies (°C) for May, 1965.

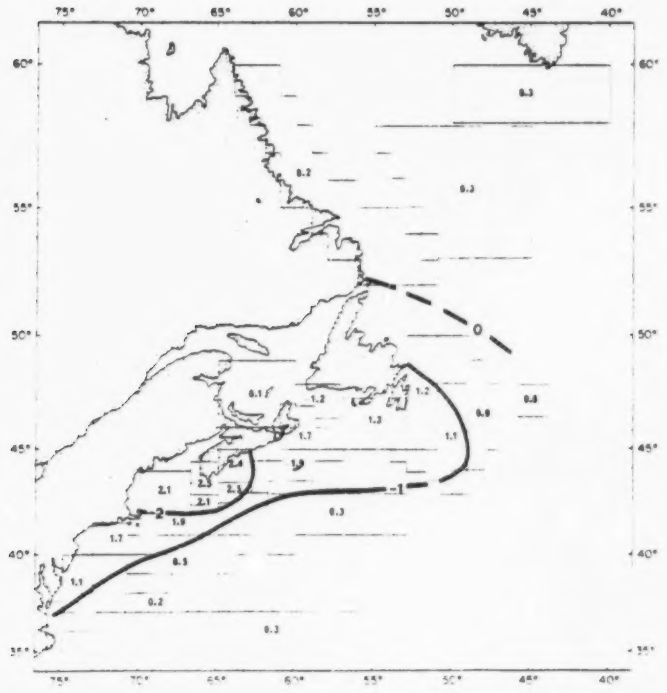

Figure 26(f) Map of GSST anomalies (°C) for June, 1965.

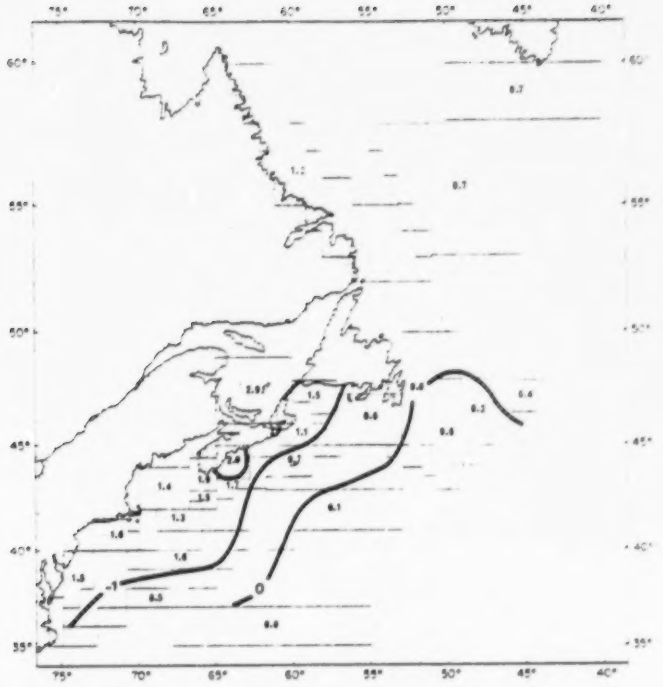

Figure 26(g) Map of GSST anomalies (°C) for July, 1965.

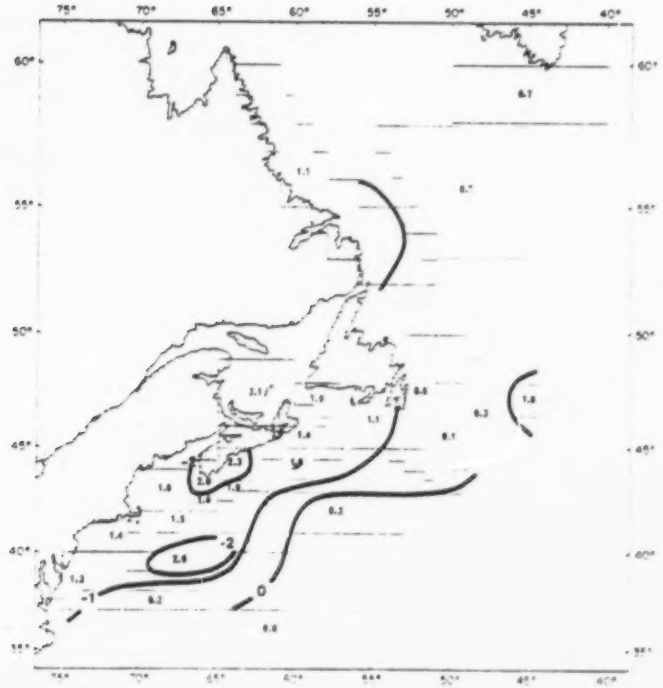

Figure 26(h) Map of GSST anomalies (°C) for August, 1965.

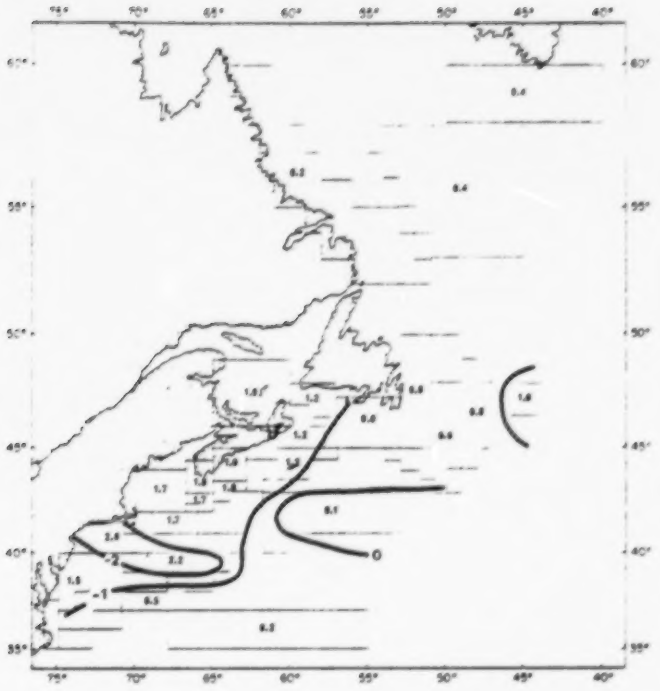

Figure 26(i) Map of GSST anomalies (°C) for September, 1965.

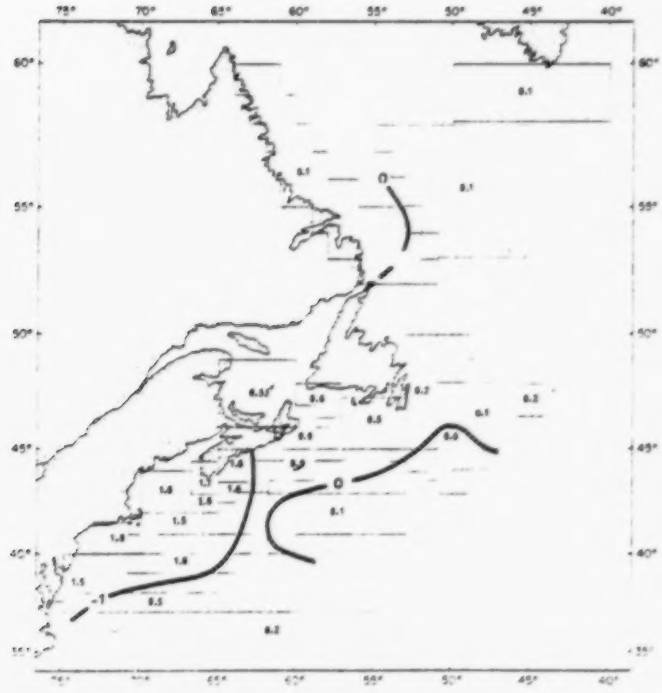

Figure 26(j) Map of GSST anomalies (°C) for October, 1965.

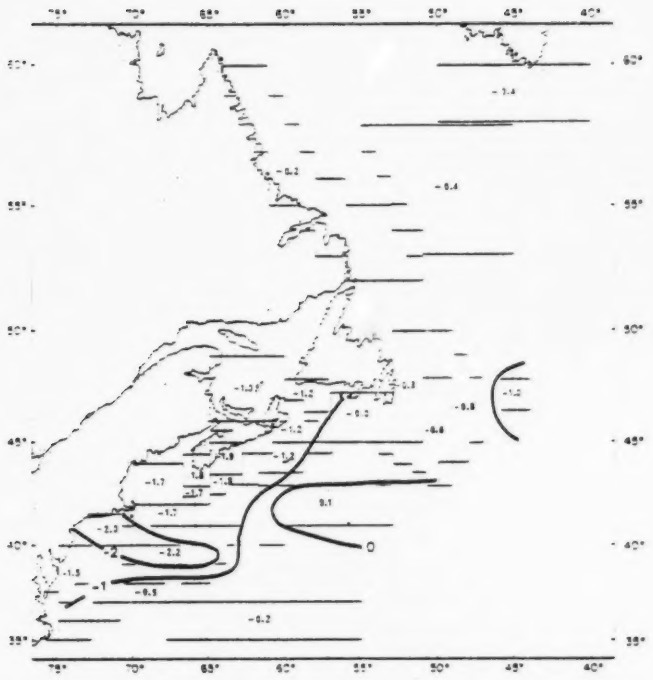

Figure 26(k) Map of GSST anomalies (°C) for November, 1965.

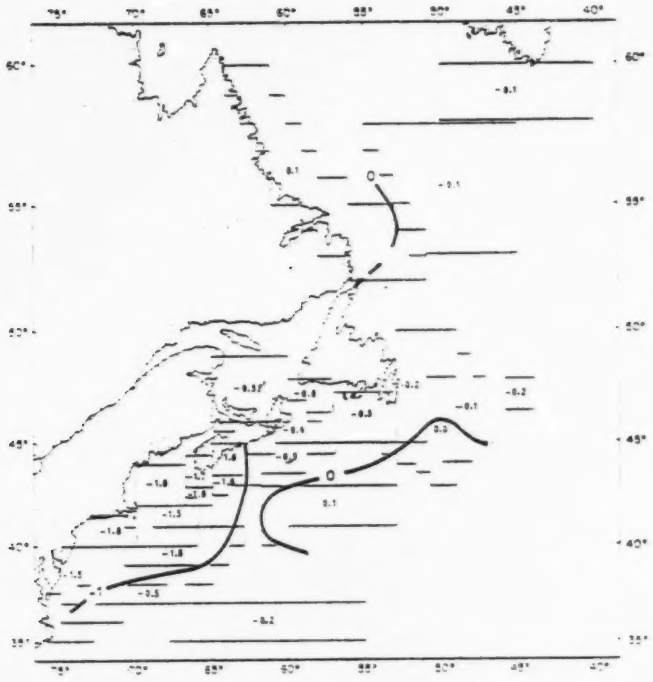

Figure 26(l) Map of GSST anomalies (°C) for December, 1965.

APPENDIX A

EOF ANALYSIS

The EOF results are given in LT for OEOF's (N) (correlation matrix) and below for OEOF (N x 12), OEOF (N x 3) and complex EOF's CEOF (N x 12), all based on the covariance matrix.

TABLE A.1 The Percentage of the total variance 'explained' by the first three modes, OEOF (N x 12).

Mode	%	Comments
1	28	uniform
2	16	tilt between GB & MAB

TABLE A.2 as for Table A.1, except by season, OEOF (N) (covariance).

	Mode	%	Comments
winter	1	31	uniform rise/fall
	2	22	tilt between GB and MAB
	3	9	
spring	1	40	uniform rise/fall
	2	20	tilt
	3	7	
summer	1	32	uniform
	2	19	tilt
	3	9	
autumn	1	27	southward streaming
	2	20	tilt
	3	11	

TABLE A.3. As for Table A.2, except OEOF (N x 3).

	Mode	%	Comments
winter	1	31	
	2	15	
	3	10	
spring	1	32	
	2	16	
	3	9	
summer	1	27	
	2	18	
	3	9	
autumn	1	28	
	2	18	
	3	7	

TABLE A.4 CEOF's (N x 12) for 10 SST areas (Figure 12). The CEOF modes are calculated for various frequency bands. Each band captures a percentage of the total variance; each mode within a band 'explains' a certain percentage of the variance for the band.

BAND	%	Mode	%	Comments
2y	65%	1	47	little progression
		2	21	tilt standing wave
		3	15	
1y	23%	1	33	progression noticeable N to S
		2	23	tilt standing
		3	14	
0.5	12%	1	30	complicated
		2	17	
		3	15	

TABLE A.5 as for Table A.4, except for 24 SST areas.

BAND	%	Mode	%	Comments
2y	64%	1	46	little propagation
		2	20	tilt standing wave
		3	10	
1y	23%	1	31	some evidence of progression
		2	17	tilt standing
		3	9	
0.5y	13%	1	26	
		2	13	standing
		3	10	

Four features may be noted: (1) Overall there is a consistency about the results, including consistency between the standing wave and progression wave analyses. (2) Although modes 1 and 2 are present at low frequencies, mode 2 seems to persist more strongly than mode 1 at higher frequencies. (3) The consistency between standing wave and progression wave analyses, or in other words, the dominance of standing waves and the weakness of phase lag differences in the complex EOF results are taken as justification for choosing the simpler path of using ordinary deseasonalized EOF's in the initial reconstruction of the SST field. (4) Table A.2 and A.3 may be interpreted to differ solely in the influence of wind fluctuations of time scale, 2 to 6 months. These are influential in the (N x 3) results and smoothed out in the (N) results. Comparing Tables A.2 and A.3 shows that these wind fluctuations are disruptive of regional coherence in winter (second mode) in spring (first and second modes) and in summer (first mode).

APPENDIX B

RELATIONSHIP BETWEEN SST ANOMALY FIELD AND WIND

To test the hypothesis that atmospheric forcing is an important driver of SST anomalies, the main approach to be pursued in future work planned by our group is a comparison between the EOF modes of SST and those of atmospheric pressure. The questions to be addressed there include: How much of the SST variance and spatial structure can be accounted for by the structure of the atmospheric field? Is the relationship between wind and SST a function of season? Which drives which? What is the structure of that fraction of the SST signal which is not coherent with atmospheric pressure? Is it an advective signal?

As a preliminary approach, the correlations between geostrophic winds (derived from atmospheric pressure distributions) and 'geophysical-scale' SST's (GSST's) are examined. GSST's, it will be recalled, are spatially-smoothed versions of the actual SST's, reconstructed from EOF's and emphasizing the coherent patterns over incoherent variability. Focusing on the Offshore Labrador Current and West Grand Bank SST areas, correlations between SST and wind and GSST and wind are presented in Table B.1 for Grand Banks seasonally averaged geostrophic winds. The results are: that correlations involving winter winds are much stronger than those for other seasons: that correlations are slightly stronger between winds and GSST's than between winds and SST's; that correlations with winds are stronger for West Grand Banks than for Offshore Labrador Current GSST's: that in the latter case the correlation is somewhat increased with a lag of one season i.e. winter winds versus spring GSST's: and that for both locations cool SST's are most strongly associated with (cool) winds from the northwest.

The conclusions from this preliminary exercise are that GSST's match the geostrophic wind field slightly better than SST's (i.e. the large scale variations

emphasized in both tend to be coherent) and more importantly, that winter winds can 'explain' up to 59% of winter or spring GSST's. For these seasons, winds seem to be a dominant driving force for Grand Banks SST's.

TABLE B.1 CORRELATIONS BETWEEN SEASONAL WINDS AND SEASONAL SST'S AND GSST'S FOR WEST GRAND BANK AND OFFSHORE LABRADOR CURRENT AREAS, 1950-1980.

AREA	GSST Maximum Correlation (Wind Bearing)	SST Maximum Correlation (Wind Bearing)
West Grand Bank		
winter winds; winter SST	-.77 (130°)	-.70 (140°)
winter winds; spring SST	-.76 (135°)	-.71 (140°)
spring winds; spring SST	-.50 (140°)	-.49 (140°)
spring winds; summer SST	-.37 (120°)	-.37 (120°)
summer winds; summer SST	.29 (140°)	-.36 (090°)
summer winds; autumn SST	-.12	-.22
autumn winds; autumn SST	-.49 (100°)	-.43 (110°)
Offshore Labrador Current		
winter winds; winter SST	-.61 (110°)	-.27
winter winds; spring SST	-.67 (125°)	-.62 (120°)
spring winds; spring SST	-.41 (140°)	-.34 (140°)
spring winds; summer SST	-.18 (130°)	-.16 (120°)
summer winds; summer SST	-.18 (130°)	-.16 (120°)
summer winds; autumn SST	.15	.05
autumn winds; autumn SST	-.38 (145°)	-.21 (110°)

APPENDIX C

RELATIONSHIP BETWEEN SST ANOMALY FIELD AND RIVER RUNOFF

This discussion pertains to the downstream effects of the St. Lawrence rivers and not necessarily to those of the Hudson Bay river.

The half-power period of the St. Lawrence river runoff is 43 months (as determined however from the power spectrum of an extremely non-stationary signal - the variance in spring is much larger than in winter). This exceeds the half-power periods of the SST's and the winds, and even those of the first and second mode OEOF's. Part of this dominance of long periods in runoff must arise because aquifers, rivers, lakes and particularly lakes with hydro-dams serve to smooth the precipitation (meteorological) signal. That this long median time-scale is not repeated in SST areas downstream e.g. Gulf of St. Lawrence, Eastern Shore suggests that drivers e.g. winds with smaller time scales are having a dominating effect. That larger median time scales emerge in the vicinity of the Gulf of Maine may be due to the 'smoothing' role played by tidal mixing and/or recirculation there.

In LT there is weak evidence that lagged correlations solely among SST's manifest the river advective effect on coastal waters of the Scotian Shelf. Again this suggests that the river effect (as well as being strongly low-passed) is confounded with others in the SST signals. A clearer relationship between runoff and downstream SST's was demonstrated by Sutcliffe et al. (1976). How are these two perspectives to be rationalized? Sutcliffe et al. (1976) presented correlations month by month between runoff and shore station temperatures. However, their monthly values were three-year running means e.g. over July for three consecutive years. Given the fact that half-power periods are four to six months for winds and 43 months for runoff, the smoothing effect of this three-year running mean would

bear much more strongly on wind processes than on runoff processes. This smoothing suppressed the wind effects, leaving exposed the runoff effects on SST (however see Koslow et al., 1985).

A clear and significant result for LT was that Scotian Shelf SST's exhibit a correlation peak between winter and summer/autumn. Our interpretation is that the runoff effect is such as to reinforce six months later the SST anomalies established during the previous winter by winds.

Natural confounding of the river effect with those of other forcing mechanisms is not likely to be resolved through the EOF technique alone i.e. without in some way discriminating against other effects. By its design, synchronous components of all forcing mechanisms would be included in that first mode. The OEOF results show the first mode to extract considerably more variance (up to twice as much) than the second mode. This relatively strong first mode may be the product of a combination of mechanisms, themselves partially synchronized, rather than of a single dominant mechanism. The EOF and lagged correlation results are consistent with the hypothesis that the river is not independent of other forcing mechanisms (such as the meteorological conditions) i.e. is partially correlated or synchronized. Clearly the EOF technique is more suitable for uncovering the prevailing spatial and temporal scales than for resolving related effects.

The geophysical scale reconstruction of the SST field, using the EOF results, enhances the dominant patterns i.e. the combination of effects which are extracted as the dominant modes. Thus, if the river effect is confounded with, for example, the meteorological effects, it is going to remain confounded through the GSST analysis. As anticipated, the GSST's reveal no very persistent coastal advective pattern during the autumn of 1951, a season when due to extreme freshet

such a pattern might have been expected. Nor in the autumn of 1965, after a very low river freshet, is a progressive negative anomaly reconstructed along the coast of Nova Scotia. Again, the implication is that both in the SST data and in the GSST reconstruction, the local air-sea heat transfers, the net radiation input and the runoff effects are confounded and not easily separable.

A final negative result adds further support for the impression that the unsmoothed SST's and GSST's reflect combinations of driving influences. It was surmised in the unlikely event that meteorological effects were separable from river effects through EOF's, that the meteorological effects would be expressed by the higher modes. The complement of the first-mode-only GSST's ($GSST_1$) could be expected to capture the river advective effect in this (unlikely) case. There is some very weak, not convincing suggestion (Table C.1) of a progressive negative anomaly in the autumn of 1965, and even less suggestion of a progressive positive anomaly in 1951, pointing to the interpretation that the river effect is not being separated efficiently from the meteorological signal in these analyses.

In summary, results are all consistent. They point to the perspective that the drivers are linked, lagged, and reinforcing that the dominant EOF mode therefore reflects both meteorological (presumably the major driver) and river advective (presumably a secondary driver) influences: and that neither lagged cross-correlations on SST's nor GSST's nor the complement of GSST's can separate the river from the meteorological effects, but that judicious smoothing can.

APPENDIX D

RELATIONSHIP BETWEEN SST ANOMALY FIELD AND OFFSHORE FORCING

We have not advanced the understanding of the role of offshore forcing except to point out (in LT) that the St. Lawrence rivers runoff is correlated with the Slope Water SST. It is suggested that the structure of that fraction of the SST field which is not coherent with atmospheric pressure might provide insights on offshore effects.

TABLE C.1 COMPARISON OF MONTHLY MEDIAN OBSERVED ANOMALIES OF SST AND FIRST-MODE-ONLY GSST FOR JANUARY, 1951 TO APRIL, 1952 AND JANUARY, 1965 TO APRIL, 1966 FOR SIX OF THE 24 AREAS

		1951												1952			
		J	F	M	A	M	J	J	A	S	O	N	D	J	F	M	A
SBL	$GSST_1$	2.1	2.0	2.3	2.3	1.9	1.2	1.6	1.9	2.0	0.6	1.3	1.4	1.1	1.6	1.2	1.5
	Actual	3.0	2.2	1.6	2.8	1.9	3.3	2.4	1.6	2.0	.3	1.1	1.2	1.3	1.6	1.1	1.1
	Residue	.9	.2	- .7	.5	0	2.1	.8	- .3	0	- .3	- .2	- .2	.2	0	- .1	- .4
ESS	$GSST_1$	2.0	1.9	2.2	2.2	1.8	1.2	1.6	1.8	1.9	0.6	1.3	1.3	1.1	1.5	1.1	1.4
	Actual	3.2	1.7	1.7	2.5	1.1	.3	2.5	1.0	1.8	1.1	1.1	1.5	.4	2.8	1.7	2.5
	Residue	1.2	- .2	- .5	.3	- .7	- .9	.9	- .8	- .1	.5	- .2	.2	- .7	1.3	.6	1.1
SS	$GSST_1$	2.9	2.7	3.2	3.2	2.6	1.7	2.3	2.6	2.7	0.8	1.8	1.9	1.5	2.2	1.6	2.0
	Actual	4.0	3.7	3.5	2.3	1.0	.5	2.9	3.3	2.4	.4	1.0	1.2	1.7	3.1	2.4	2.3
	Residue	1.1	1.0	.3	- .9	-1.6	-1.2	.6	.7	- .3	- .4	- .8	- .7	.2	.9	.8	.3
Y	$GSST_1$	2.6	2.4	2.8	2.8	2.2	1.5	2.0	2.3	2.4	0.7	1.6	1.6	1.3	1.9	1.4	1.8
	Actual	2.6	2.5	2.3	3.4	2.6	0.6	3.6	4.3	1.2	.1	1.2	1.0	- .8	3.1	-1.5	2.3
	Residue	0	.1	- .5	.6	.4	- .9	1.6	2.0	-1.2	- .6	- .4	- .6	-2.1	1.2	-2.9	.5
GOM	$GSST_1$	2.3	2.2	2.5	2.5	2.0	1.3	1.8	2.0	2.1	0.7	1.5	1.5	1.2	1.7	1.3	1.6
	Actual	1.5	1.8	1.7	2.0	2.1	1.0	1.2	1.4	1.8	1.0	1.0	1.3	2.1	2.9	2.2	.9
	Residue	- .8	- .4	- .8	- .5	+ .1	- .3	- .6	- .6	- .3	+ .3	- .5	- .2	0.9	1.2	0.9	- .7
GB	$GSST_1$	2.4	2.2	2.6	2.6	2.1	1.4	1.8	2.1	2.2	0.7	1.5	1.5	1.2	1.8	1.3	1.7
	Actual	1.7	1.9	2.2	1.9	3.6	1.3	2.0	1.5	3.4	1.4	2.1	2.3	1.1	1.9	2.7	1.9
	Residue	- .9	- .2	- .2	- .7	-1.6	- .2	0	- .7	-1.2	0.7	0.6	0.9	- .3	0.2	1.6	0.2

		1965												1966			
		J	F	M	A	M	J	J	A	S	O	N	D	J	F	M	A
SBL	$GSST_1$	-1.2	-0.9	-0.7	-1.0	-1.3	-1.4	-1.6	-1.6	-1.3	-1.5	-1.4	-1.1	-1.2	-1.0	-0.8	-0.7
	Actual	- .8	- .6	-1.1	-1.1	-2.6	-2.5	-1.7	- .4	- .6	-1.0	.1	-1.0	-1.1	-0.2	.3	- .2
	Residue	.4	.3	- .4	- .1	-1.3	-1.1	- .1	1.2	.7	.5	1.5	.1	.1	.3	1.1	.5
ESS	$GSST_1$	-1.1	-0.9	-0.7	-0.9	-1.2	-1.4	-1.5	-1.5	-1.2	-1.5	-1.4	-1.1	-1.2	-0.9	-0.7	-0.7
	Actual	- .7	- .4	0	- .5	-1.8	-1.7	-1.6	- .8	-1.9	-1.4	-1.1	-1.4	-1.2	-0.8	0	- .8
	Residue	.4	.5	.7	.4	- .6	- .3	- .1	- .3	.3	.1	.3	- .3	0	.1	.7	- .1
SS	$GSST_1$	-1.6	-1.2	-1.0	-1.4	-1.7	-2.0	+2.2	-2.2	-1.8	-2.1	-2.0	-1.6	-1.7	-1.3	-1.1	-1.0
	Actual	-1.1	- .9	- .9	-1.5	-2.0	-2.8	-3.4	-6.3	-0.9	-1.8	-2.5	-2.0	-1.5	-1.5	-1.3	-0.7
	Residue	.5	.3	.1	- .1	- .3	- .8	-1.2	-4.1	.9	.3	.5	- .4	.2	- .2	- .2	.3
Y	$GSST_1$	-1.4	-1.1	-0.9	-1.2	-1.5	-1.7	-1.9	-1.9	-1.5	-1.9	-1.7	-1.4	-1.5	-1.2	-0.9	-0.9
	Actual	- .8	- .5	- .6	- .7	-1.6	-2.7	-3.0	-3.2	-4.1	-3.6	-3.0	-1.8	- .3	- .4	- .3	- .5
	Residue	.6	.6	.3	.5	- .1	-1.0	-1.1	-1.3	-2.6	-1.7	-1.3	- .4	1.2	.8	.6	.4
GOM	$GSST_1$	-1.3	-1.0	-0.8	-1.1	-1.4	-1.6	-1.7	-1.7	-1.4	-1.7	-1.6	-1.2	-1.3	-1.0	-0.8	-0.8
	Actual	-1.8	-2.1	-1.7	-1.9	-2.3	-1.2	-3.3	-3.6	-1.5	-1.9	-2.9	-2.0	-1.7	-1.3	-1.7	-1.4
	Residue	- .5	-1.1	- .9	- .8	- .9	.4	-1.6	1.9	- .1	- .2	-1.3	- .8	- .4	- .3	- .9	- .6
GB	$GSST_1$	-1.3	-1.0	-0.8	-1.1	-1.4	-1.6	-1.8	-1.8	-1.4	-1.7	-1.6	-1.3	-1.4	-1.1	-0.9	-0.8
	Actual	-1.1	-1.5	-1.7	-2.3	-2.5	-1.9	-1.2	-1.2	-1.7	-1.3	-1.8	-1.8	-1.7	-1.8	-1.5	-1.3
	Residue	.7	- .5	- .9	-1.2	-1.1	- .3	.6	.6	- .3	.4	- .2	- .5	- .3	- .7	- .6	- .5